RECLAMATION
Managing Water in the West

Detecting, Interpreting, and Modeling Hydrologic Extremes to Support Flexible Water Management and Planning

Research and Development Office
Science and Technology Program
(Final Report) ST-2019-1782-01

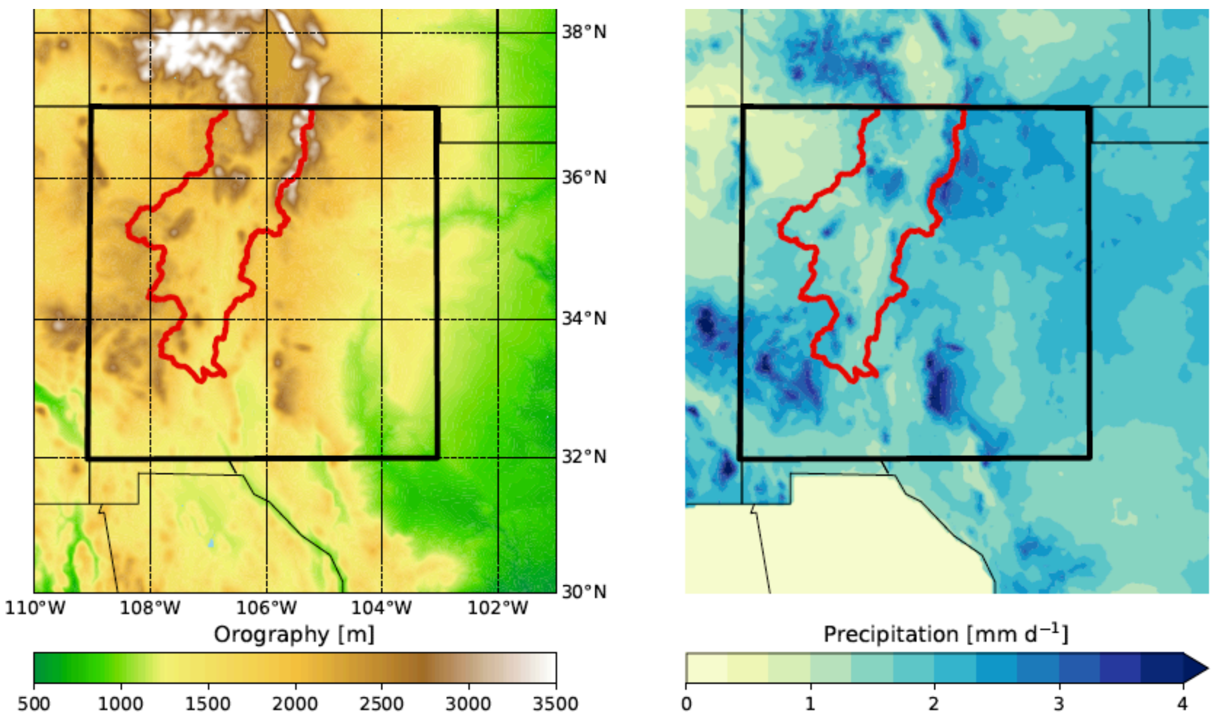

U.S. Department of the Interior
Bureau of Reclamation
Research and Development Office

Sept. 2019

Mission Statements

Protecting America's Great Outdoors and Powering Our Future

The Department of the Interior protects and manages the Nation's natural resources and cultural heritage; provides scientific and other information about those resources; and honors its trust responsibilities or special commitments to American Indians, Alaska Natives, and affiliated island communities.

REPORT DOCUMENTATION PAGE

Form Approved
OMB No. 0704-0188

T1. REPORT DATE:
SEPTEMBER 2019

T2. REPORT TYPE:
RESEARCH

T3. DATES COVERED

T4. TITLE AND SUBTITLE
Detecting, Interpreting, and Modeling Hydrologic Extremes to Support Flexible Water Management and Planning

5a. CONTRACT NUMBER

5b. GRANT NUMBER

5c. PROGRAM ELEMENT NUMBER
1541 (S&T)

6. AUTHOR(S)
Dagmar Llewellyn, Bureau of Reclamation, Albuquerque Area Office; 505-462-3594, dllewellyn@usbr.gov
Erin Towler, National Center for Atmospheric Research, Boulder, CO, 303-497-2724, towler@ucar.edu
Andreas Prein, National Center for Atmospheric Research, Boulder, CO, 303-497-8200, prein@ucar.edu

PARTICIPANT(S)
Maryam Pournasiri Poshtiri, formerly of National Center for Atmospheric Research, Boulder CO
Lucas Barrett, Bureau of Reclamation, Albuquerque Area Office
Rick Young, Bureau of Reclamation, Albuquerque Area Office
Ariane Pinson, US Army Corps of Engineers, Albuquerque District
Eric Gilleland, National Center for Atmospheric Research, Boulder, CO

5d. PROJECT NUMBER
ST-2019-1782-01

5e. TASK NUMBER

5f. WORK UNIT NUMBER
ALB-402

7. PERFORMING ORGANIZATION NAME(S) AND ADDRESS(ES)
Albuquerque Area Office
555 Broadway Blvd. NE, Suite 100, Albuquerque, NM 87102

Mesoscale and Microscale Meteorology Laboratory
National Center for Atmospheric Research
P.O. Box 3000, Boulder CO 80307

8. PERFORMING ORGANIZATION REPORT NUMBER

9. SPONSORING / MONITORING AGENCY NAME(S) AND ADDRESS(ES)
Research and Development Office
U.S. Department of the Interior, Bureau of Reclamation,
PO Box 25007, Denver CO 80225-0007

10. SPONSOR/MONITOR'S ACRONYM(S)
R&D: Research and Development Office
BOR/USBR: Bureau of Reclamation
DOI: Department of the Interior

11. SPONSOR/MONITOR'S REPORT NUMBER(S)
ST-2019-1782-01

12. DISTRIBUTION / AVAILABILITY STATEMENT
Final report can be downloaded from Reclamation's website: https://www.usbr.gov/research/

13. SUPPLEMENTARY NOTES

14. ABSTRACT *(Maximum 200 words)*
This research has four main components: (1) Examine the variability and trends of precipitation extremes, (2) Identify weather types associated with precipitation anomalies, (3) Statistically model extreme precipitation using

the weather type information, and (4) Develop a generalized framework to identify intersections between changing hydrology and water management. The approach was developed and demonstrated in New Mexico river basins (e.g., Rio Grande and Pecos), but the general approaches are transferable Reclamation-wide.

15. SUBJECT TERMS Precipitation extremes, Monsoon, New Mexico, Extreme Value Theory, Weather Types					
16. SECURITY CLASSIFICATION OF:			**17. LIMITATION OF ABSTRACT** U	**18. NUMBER OF PAGES**	**19a. NAME OF RESPONSIBLE PERSON** Dagmar Llewellyn
a. REPORT U	**b. ABSTRACT** U	**c. THIS PAGE** U			**19b. TELEPHONE NUMBER** 505-462-3594

BUREAU OF RECLAMATION

Research and Development Office
Science and Technology Program

(Final Report) ST-2019-1782-01

Detecting, Interpreting, and Modeling Hydrologic Extremes to Support Flexible Water Management and Planning

Prepared by: Erin Towler
Project Scientist, NCAR

Checked by: Dagmar Llewellyn
Hydrologist, Albuquerque Area Office, UC Region

Checked by: Lucas Barrett
Hydrologist, Albuquerque Area Office, UC Region

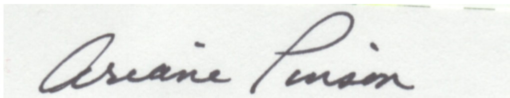

Peer Review: Ariane Pinson
Climate Science Specialist, US Army Corps of Engineers, Albuquerque District

Peer Review: Kenneth Nowak
Water Availability Research Coordinator, Research and Development Office

For Reclamation disseminated reports, a disclaimer is required for final reports and other research products, this language can be found in the peer review policy:
This document has been reviewed under the Research and Development Office Discretionary peer review process https://www.usbr.gov/research/peer_review.pdf consistent with Reclamation's Peer Review Policy CMP P14. It does not represent and should not be construed to represent Reclamation's determination, concurrence, or policy.

Cover Image: The red outline is the watershed of the Rio Grande above Elephant Butte Reservoir in New Mexico (bold black line). Figure on the left shows topography and the figure on the right shows average July through September daily precipitation (1981-2018).

Executive Summary

Problem Statement

Precipitation and streamflow extremes are critical parameters in Reclamation's water resources planning, due to both the management threats and opportunities that they provide, as well as their importance to ecosystems and endangered species. Given climate variability and change, Reclamation needs non-stationary tools to help it characterize these extremes, to improve its water management and planning.

Research Activities and Results

This project set out to investigate non-stationary tools to characterize extreme precipitation events, first by identifying the drivers of precipitation anomalies, and then by modeling their characteristics. These tools were demonstrated for monsoon precipitation in New Mexico. Monsoons represent a water source that is likely going to continue to grow in importance for water management in the U.S. Southwest, but is also a water source that has been challenging to forecast seasonally and to project into the future.

This research has four main components: (1) Examine the variability and trends of precipitation extremes, (2) Identify weather types associated with precipitation anomalies, (3) Statistically model extreme precipitation using the weather type information, and (4) Develop a generalized framework to identify intersections between changing hydrology and water management. The components are developed and demonstrated in New Mexico (NM) river basins (e.g., Rio Grande and Pecos), but the general approaches are transferable Reclamation-wide.

Weather types (WTs) are shown to be an effective way to characterize the large-scale conditions that drive precipitation variability and trends. Coupling this dynamical understanding with statistical approaches based on Extreme Value Theory allowed for the modeling of the characteristics of extreme precipitation events, such as the frequency and magnitude, which are of interest to water managers. These tools were applied to observations to understand recent variability and trends, and were also used with an ensemble of climate model projections to characterize likely future changes in extreme precipitation events associated with NM monsoons.

Future Plans

From these encouraging results, two new research questions arose: First, can WTs be used to forecast monsoon precipitation on other time scales, such as from seasonal to decadal? To answer this, there is a need to evaluate the skill of the WT circulation patterns in forecast products. Second, what is the potential value of monsoon forecast information for water managers? It would be useful to develop a systematic framework to test a range of probabilistic forecast scenarios for a water system, with the goal of assessing the sensitivity of the watershed hydrology and management to monsoon predictability. These research questions are complementary to ongoing Reclamation activities that are focused on improving snowmelt-runoff forecasts.

Contents

Main Report

Problem Statement

Precipitation and streamflow extremes are critical parameters in Reclamation's water resources planning, due to both the management threats and opportunities that they provide, as well as their importance to ecosystems and endangered species. Given climate variability and change, Reclamation needs non-stationary tools to help it characterize these extremes, to improve its water management and planning. This research was guided by two overarching questions and associated hypotheses:

(1) How can we better detect and interpret the variability and trends of hydrologic extremes? *We hypothesize that weather types can help to interpret the variability and trends detected in historical hydrologic records.*

(2) How can we incorporate this understanding into non-stationary tools that support flexible water management and improved planning? *We hypothesize that statistical tools, such as Extreme Value Theory (EVT), can be used with weather type information to enable non-stationary estimates of the frequency and magnitude of extreme threshold exceedances.*

Research Activities and Results

This research has four main components: (1) Examine the variability and trends of precipitation extremes, (2) Identify weather types associated with precipitation anomalies, (3) Statistically model extreme precipitation using the weather type information, and (4) Develop a generalized framework to identify intersections between changing hydrology and water management. The components are developed and demonstrated in New Mexico (NM) river basins (e.g., Rio Grande and Pecos), but the general approaches are transferable Reclamation-wide. The main approach and findings from each component are detailed below.

For the first component, we examine recent variability and trends in precipitation characteristics within the state of New Mexico and southern Colorado, with a focus on the Rio Grande and Pecos basins. To determine how changing precipitation could potentially help to mitigate decreasing water supply, we examine both magnitude and frequency of daily precipitation characteristics for the warm season, defined here as June 1 to October 31 (June - October) and individual months therein, with a focus on the upper quantiles and extremes within the period 1981 to 2017. We find that the dominant sign of the precipitation trend depends on the season/month examined. Negative trends dominate if we examine the entire warm season (i.e., June-October), as well as during the individual month of June, and August, while positive trends dominate July and for some September indicators. However, the majority of locations in the study area do not show any significant trends. The increasing trends for the July indicators show the most potential for water supply, with the location of these significantly positive trends mainly concentrated in the southeastern and eastern part of the study region, relevant to the Pecos basin. The frequency of days above the 99th daily precipitation quantile for September also shows increasing trends at some southern and southeastern locations, but this heavy precipitation could be difficult to capture for water supply. However, across most of the upper quantile and extremes characteristics examined, we find that significant trends are more detectable in the frequency indicators than in the magnitude indicators. The outcomes of this component were published in the proceedings of the Western Snow Conference. This publication is provided in Appendix A: "Extremes of opportunity: Examining recent trends in warm season extreme precipitation for New Mexico river basins," (Pournasiri Poshtiri et al. 2018).

The second component uses a clustering algorithm to identify distinct atmospheric circulation patterns, or weather types (WTs), associated with NM precipitation anomalies. To identify the WTs, three large-scale variables (precipitable water, sea level pressure, and wind speed) are selected and examined over the state of NM. Four hydrologically important weather types that occur during NM's warm season (June through October) are identified as follows: WT1 and WT2 are associated with dry conditions, while WT3 and WT4 are associated with wet conditions. WT4 represents the North American Monsoon and contributes more than 50% to the warm season precipitation, including the majority of the heaviest precipitation events (~60%). WT3 contributes about a third of the warm season precipitation, and has less intense precipitation than WT4. The analysis shows that NM has experienced a decrease in average daily precipitation from 1980 to 2010, mostly caused by a change to more frequent dry weather types and decreasing precipitation rates in two of the four WTs. We examine WT frequency in a large ensemble climate projection dataset, and find that the model is able to reproduce the WT climatology well, despite not being able to resolve the actual monsoon processes and precipitation. In the future, the large ensemble median shows a decrease in the frequency of WT4 days (the wetter monsoon days) until about 2050 (-5%), mostly in August, September, and October. This is followed by increasing frequency until the end of the century (+15%), mostly occurring in June, July, September, and October. The processes that trigger these nonlinear changes are unclear but additional model experiments show that they are caused by increasing greenhouse gas forcing rather than changes in aerosols or land use. However, both large-scale dynamic and thermodynamic changes suggest more monsoonal rainfall in New Mexico in the second half of the century. A manuscript containing pertinent data and results pertaining to this component has been finalized and submitted to a refereed journal. The title is: "The Changing Character of the North American Monsoon and its Impacts on New Mexico's Precipitation", by Andreas F. Prein. The principal investigator of this work will update this section to include the submitted manuscript once the journal peer review process has been resolved and information is ready for public dissemination. There is a placeholder for this manuscript in Appendix B.

The third component was to statistically model extreme precipitation using the WT information. An Extreme Value Theory (EVT) model is developed using daily precipitation extremes in the Rio Grande Watershed. Specifically, the Point Process (PP) approach is used, which is a unified framework for modeling the frequency and magnitude of extremes above a threshold using the Poisson and Generalized Pareto (GP) models, respectively. Incorporating the wet WT covariates in the PP model improves the fit: the number of WT4 days is included as a covariate in the location parameter and the number of WT3 days in the scale parameter. When the PP model is applied in a downscaling context using the large ensemble climate projection dataset, the frequency of having an extreme precipitation event increases after 2050, which is consistent with the increase in WT4 days. No change is seen, however, in the magnitude of extremes. The accepted manuscript containing pertinent data and results pertaining to this component is included in Appendix C: "Extreme-value analysis for the characterization of extremes in water resources: A generalized workflow and case study on New Mexico monsoon precipitation", by Erin Towler, Dagmar Llewellyn, Andreas Prein, and Eric Gilleland.

The fourth component was to develop a generalized approach to identifying potential intersections between changing hydrology and water management. The first step is to articulate management vulnerabilities and opportunities. The second step is to quantify current water contributions from sources that may provide the hydrologic opportunity. Next, it is important to identify key climatic and atmospheric drivers of the hydrologic opportunity, and finally, it is necessary to explore the opportunity-management nexus. The framework is demonstrated using the Middle Rio Grande Basin of New Mexico and its downstream delivery point, Elephant Butte Reservoir. In Step 1, we articulate how NM's water supplies are vulnerable to decreasing snowpack, but also that the summer monsoon season could offer a potential, currently under-developed, water supply opportunity. In Step 2 we examine historical Elephant Butte Reservoir inflows and find that although monsoon season volumes vary from year-to-year, they are an important contribution to annual water supply. Further, we find that the upper percentile inflows contribute a disproportionately larger fraction of the monsoon volume relative to their frequency of occurrence. Step 3 examines possible climate and atmospheric drivers for different characteristics of monsoon season interannual variability, finding that most monsoon inflow characteristics show a strong association with average precipitation over the contributing watershed and atmospheric precipitable water. In Step 4 we suggest how this information could be integrated into existing planning and operations for the Rio Grande Basin. The outcome of this component was peer reviewed and published in the proceedings of the Federal Interagency Sedimentation and Hydrologic Modeling Conference (SEDHYD). This publication is provided in Appendix D: "Extremes of Opportunity? A generalized approach to identify intersections between changing hydrology and water management," (Towler et al. 2019).

Appendix E to this report provides a complete list of the research products for each component, including the papers, presentations, and outreach efforts.

Summary Findings and Future Plans

This project set out to investigate non-stationary tools to characterize extreme precipitation events, first by identifying the drivers of precipitation anomalies, and then by modeling their characteristics. These tools were demonstrated for monsoon precipitation in New Mexico. Monsoons represent a water source that is likely going to continue to grow in importance for water management in the U.S. Southwest, but is also a water source that has been challenging to forecast seasonally and to project into the future.

WTs are shown to be an effective way to characterize the large-scale conditions that drive precipitation variability and trends. Coupling this dynamical understanding with statistical approaches based on Extreme Value Theory allowed for the modeling of the characteristics of extreme precipitation events, such as the frequency and magnitude, which are of interest to water managers. These tools were applied to observations to understand recent variability and trends, and were also used with an ensemble of climate model projections to characterize likely future changes in extreme precipitation events associated with monsoons in New Mexico.

From these encouraging results, two new research questions arose: First, can WTs be used to forecast monsoon precipitation on other time scales, such as from seasonal to decadal? To answer this question, there is a need to evaluate the skill of the WT circulation patterns in forecast products. This could be assessed using existing seasonal forecast ensembles, such as the North American Multi-Model Ensemble (NMME). Second, what is the potential value of monsoon forecast information for water managers? It would be useful to develop a systematic framework to test a range of probabilistic forecast scenarios for a water system, with the goal of assessing the sensitivity of the watershed hydrology and management to monsoon predictability. These research questions are complementary to ongoing Reclamation activities that are focused on improving snowmelt-runoff forecasts. Future plans include explicitly linking monsoon-based forecasts with spring-runoff forecasts being developed in another Reclamation-funded Science & Technology Program project, "Improving the resiliency of southwestern US water supply forecasting in the face of climate trends and variability" (S&T Project 8117), being conducted by PI Llewellyn and NCAR colleagues.

References

Pournasiri Poshtiri M, Towler E, Llewellyn D, Prein AF (2018) Extremes of opportunity: Examining recent trends in warm season extreme precipitation for New Mexico river basins, 86th Western Snow Conference, Albuquerque, NM, https://westernsnowconference.org/files/PDFs/2018Poshtiri.pdf.

Towler E, Llewellyn D, Barrett L, Young R (2019) Extremes of Opportunity? A generalized approach to identify intersections between changing hydrology and water management. Proceedings of the Federal Interagency Sedimentation and Hydrologic Modeling Conference (SEDHYD), Reno, NV, https://www.sedhyd.org/2019/openconf/modules/request.php?module=oc_program&action=view.php&id=160&file=1/160.pdf.

Appendix A – Component 1 Paper

Extremes of Opportunity: Examining Recent Trends in Warm Season Extreme Precipitation for New Mexico River Basins

Maryam Pournasiri Poshtiri[1], Erin Towler[1], Dagmar Llewellyn[2], and Andreas Prein[1]

[1] National Center for Atmospheric Research (NCAR), Boulder, CO

[2] Bureau of Reclamation, Albuquerque, NM

Paper published in the Proceedings of the Western Snow Conference 2018

Abstract

We explore recent trends in precipitation characteristics within the state of New Mexico and southern Colorado, relevant to the Rio Grande and Pecos basins, where increasing temperatures and decreasing snowpack threaten to reduce the water available for storage and use. To determine how changing precipitation could potentially help to mitigate decreasing water supply, we examine both magnitude and frequency of daily precipitation characteristics for the warm season (June - October) and individual months therein, with a focus on the upper quantiles and extremes within the period 1981 to 2017. We find that the dominant sign of the precipitation trend depends on the season/month examined. Negative trends dominate warm season, June, and August, while positive trends dominate July and for some September indicators. However, the majority of locations in the study area did not show any significant trends. The increasing trends for the July indicators show the most potential for water supply, with the location of these significantly positive trends mainly concentrated in the southeastern and eastern part of the study region. The frequency of days above the 99th daily precipitation quantile for September also shows increasing trends at some southern and southeastern locations, but this heavy precipitation could be difficult to capture for water supply. However, across most characteristics examined, we find that significant trends are more detectable in the frequency indicators than in the magnitude indicators. As such, for times and locations showing increasing trends, this suggests that water managers looking to exploit changes in precipitation might not need to plan for larger events, but rather for more frequent events.

Introduction

In many river basins in the Western United States, winter snowmelt provides the primary supply of water, with warm season precipitation as a secondary source (Serreze *et al.*, 1999). However, decreases in snowpack have already been observed (Mote *et al.*, 2005; Chavarria, 2017) and climate models project that these trends will continue (Solomon *et al.*, 2007). This suggests that warm season precipitation may provide a more substantial contribution to water supply. However, it is generally thought that increasing greenhouse gases will increase heavy precipitation. Thus, to investigate if warm season precipitation events might present opportunities to mitigate the impacts of decreasing snowmelt, it is necessary to understand the changing precipitation characteristics, especially the extremes. The goal of this paper is to investigate trends in precipitation, with a focus on the upper quantiles and extremes, to determine how changing precipitation could potentially help to mitigate the impacts of decreasing snowpack on water supply. This is of particular interest in the arid U.S. southwest, where water resources are strained (Pournasiri Poshtiri & Pal, 2016). As such, we provide a case study example relevant to New Mexico river basins, including the Rio Grande and Pecos basins, where some evidence suggests that the strength of the summer monsoon may increase (e.g., Asmerom *et al*., 2013) and there may be opportunities to exploit changes in precipitation for water management (Gutzler, 2013, Llewellyn & Vaddey, 2013).

Data and Methods

This study focuses on the state of New Mexico and southern Colorado (Longitude: 109 to 103 W & Latitude: 32 to 38 N, and see Figure 3), which includes the Rio Grande and Pecos basins. We use gridded daily precipitation data from PRISM Gridded Climate Data Group (prism.oregonstate.edu), downloadable from http://www.prism.oregonstate.edu/documents/PRISM_downloads_FTP.pdf. The 4 km daily precipitation data is processed by averaging 10 x 10 grid cells, resulting in 225 cells total. We examine data from 1981-2017, with a focus on the warm season, here defined as June through October. This is when most of the direct precipitation that falls on New Mexico is associated with summer monsoons and remnant tropical storms.

For precipitation, we examine both magnitude and frequency characteristics. For magnitude, we examine five precipitation magnitude indicators for the upper (higher value) quantiles: q50, q75, q90, q95, and q99 (i.e., the 50th percentile to the 99th percentile), as well as the average (avg) and maximum (max) values. For each magnitude indicator, we construct a time series of the daily value for each year's warm season (or individual month) in each grid cell. For frequency, we consider five thresholds of the upper quantiles (i.e., q50, q75, q90, q95, and q99), which are calculated over the entire precipitation record for the warm season (or individual month) in each grid cell. Consequently, we define the frequency indicators as the time series of the number of days above each of the thresholds in each grid cell.

To identify if there is a monotonic temporal trend in the magnitude, we use the nonparametric Mann-Kendall test (Kendall, 1975, Mann, 1945); this is done for the magnitudes for each precipitation indicator at each grid cell. To identify if there is any trend in the frequency of days above the threshold, we use Poisson regression. Poisson regression is used because the response variables are in the form of count data and are discrete (e.g., Dobson & Barnett, 2008, Fox, 2015). For both, we consider trends with p-values <0.05 as statistically significant.

Results and Discussion

In this section, we discuss the trend results, compare the trends in magnitude and frequency, and examine the spatial trend patterns.

<u>Trend Results</u>

Trend results for the precipitation indicators over the warm season (June through October) and each individual month are presented in Table 1. The tables summarize the percentage of grid cells where the precipitation trends are statistically significant (p-values <0.05). For June-October, we see that for both magnitude and frequency, for q90 and higher, the significant negative (drying) trend dominates. However, the percentages are not that high: the maximum percent of cells showing drying for the magnitude and frequency indicators are 13% and 50%, respectively. June and August show similar drying trend results. Conversely, July differs by showing more increasing trends, especially for the q50 indicators (45% and 56% for magnitude and frequency indicators, respectively). We point out that many grid cells have a q50 of zero (i.e., more than half the days don't receive any precipitation), so for this, the trend increase indicates an increase in the non-zero precipitation days. For July, we also see that positive (wetter) trends dominate all of the July frequency indicators. Most of September and October indicators don't have many cells with significant trends (many indicators detect trends at less than 5% of the grid cells), with a notable exception: in September, the q99 frequency indicator shows an increasing trend at 22% of the grid cells. However, it is important to note that the majority of locations in the study area did not show any significant trends. Further, this study focuses on trends in the recent period (1981-2017), but it has been shown that trends are dependent on time period analyzed (Pournasiri Poshtiri & Pal, 2016).

Comparing the trend in magnitude and frequency characteristics

Figure 1 compares the percent of grid cells with statistically significant negative trends between the magnitude and frequency quantile indicators. In June-October (Figure 1A), June (Figure 1B), and August (Figure 1D), we see that across quantiles, there is a higher percentage of grid cells with negative trends in frequency than in magnitude (i.e., the red bars are higher than the orange bars). There is one exception for q99 in June (Figure 1B), where magnitude (orange bar) displays a higher number of grid cells with a negative trend than frequency (red bar). In short, the trend is more detectable in the frequency of extreme precipitation rather than the magnitude, in agreement with the recent study by Mallakpour & Villarini (2017). As previously mentioned, we don't see dominant negative trends in July (Figure 1C), September (Figure 1E), nor October (Figure 1F), and this is reflected in the both frequency and magnitude bars.

We do see some positive trends for July and September (Table 1), so Figure 2 compares the percent of grid cells with statistically significant positive trends for these two months. We clearly see the dominant positive trend in July across all indicators (Figure 2A) and dominant positive trend for q50 and q99 in September (Figure 2B). This shows how in recent years, the sign of the precipitation trend is sensitive to the season or month examined. In the next section, we explore the spatial patterns of the precipitation trends during June-October as well as July and September.

Table 1. Percentage of grid cells with a statistically significant trend (p-values <0.05) for each precipitation indicator. +Sig indicates a statistically significant increasing (wetter) trend, and -Sig indicates a statistically significant decreasing (drying) trend. Bold values indicate where the percentage of grid cells is greater than 5% and is also higher than that of the opposite sign.

Characteristic	Indicator	June-October		June		July		August		September		October	
		+Sig	-Sig	+Sig	-Sig	+Sig	-Sig	+Sig	-Sig	+Sig	-Sig	+Sig	-Sig
Magnitude	avg	0.89	**5.8**	0	**24**	4.0	0	0	**17**	0	0	0	0
	q50	**19**	5.3	4.4	4.9	**45**	0	4.0	**14**	**8.4**	2.7	0	0.44
	q75	2.7	4.0	0.44	**17**	**11**	0	0	**19**	0	0.44	0	0
	q90	0	**11**	0	**27**	2.7	0	0	**20**	0	3.1	0	0
	q95	0.44	**13**	0	**28**	4.0	0	0.44	**17**	0	0.44	0	0
	q99	5.3	**8.9**	0.44	**19**	2.7	0	1.3	**10**	0.44	0.89	0.44	**6.2**
	max	3.6	**6.7**	0.44	**18**	3.6	0.44	1.8	**8.0**	1.3	1.3	0.89	**7.6**
Frequency	q50	**28**	26	8.4	**31**	**56**	0	7.6	**21**	**7.6**	**7.6**	**5.8**	0.89
	q75	3.1	**39**	3.6	**37**	**28**	3.6	0	**26**	0.44	2.7	2.7	0.89
	q90	0.89	**50**	0	**43**	**13**	5.8	0	**32**	0	4.9	0	**5.3**
	q95	0.44	**39**	0	**40**	**15**	3.1	1.3	**27**	4.9	1.3	0	**10**
	q99	5.8	**13**	0	**16**	**12**	3.6	0.89	**10**	**22**	1.8	0.89	**13**

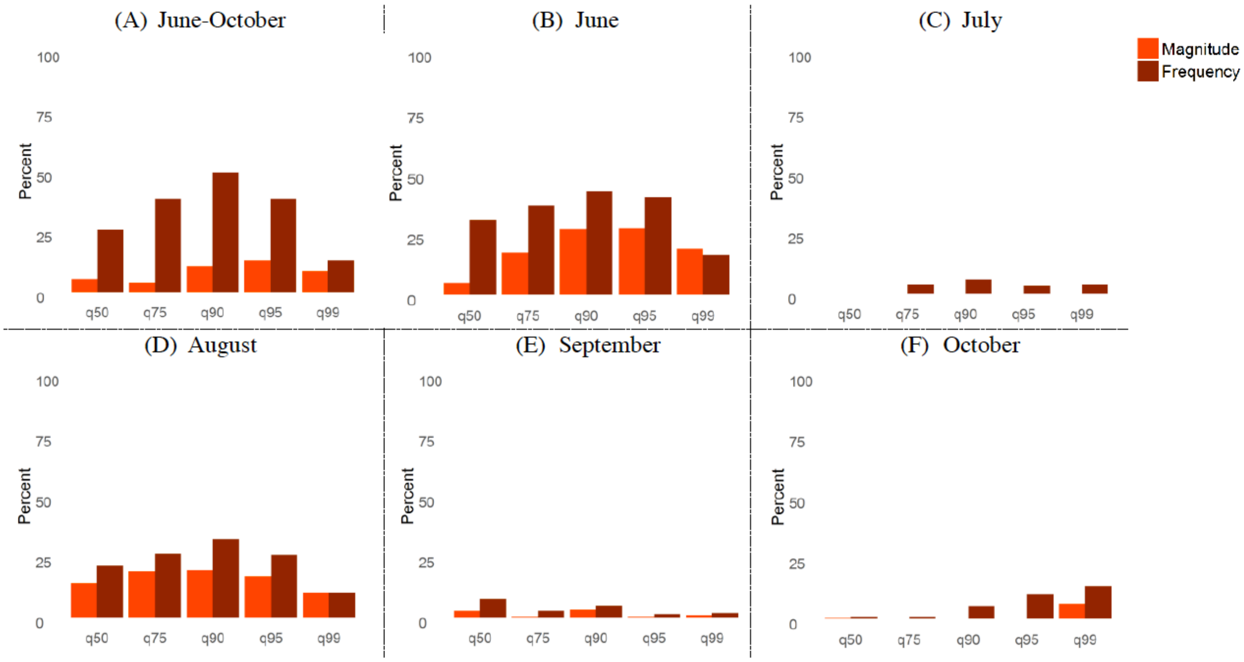

Figure 1. Percent of grid boxes with statistically significant negative (drying) trends (p-values <0.05, Table 1) for different quantiles of the magnitude and frequency precipitation indicators.

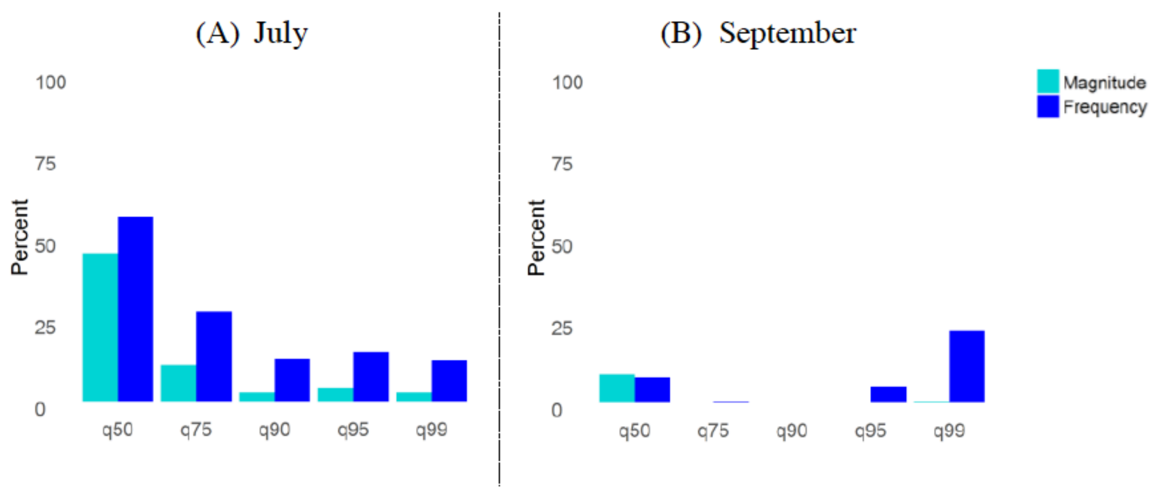

Figure 2. Percent of grid boxes with statistically significant positive (wetter) trends (p-values <0.05 , Table 1) for different quantiles of the magnitude and frequency precipitation indicators for July and September.

<u>Examining the spatial trend patterns</u>

In this section, we illustrate the spatial patterns in the magnitude and frequency of the indicators for June-October (Figure 3), July (Figure 4), and September (Figure 5) within the study region. These figures show that the spatial pattern of both increasing and decreasing trends vary across the different quantiles and seasons/months. Over the warm season (Figure 3), the regions in the northwest and southwest exhibit the strongest decreasing trends, which is more notable in frequency for q75, q90, and q95 (Figure 3 B-D). On the other hand, positive trends are observed from the southern regions to the central parts for q50 (Figure 3A), while it is concentrated in a few areas over the east for q75 (Figure 3B) and q99 (Figure 3E). In July, q50 (Figure 4A) shows positive trends over much of the domain except in the west and northwestern parts. As we move from lower quantile (i.e., q50, Figure 4A) to higher quantiles (i.e., q99, Figure 4E), the spatial coverage decreases and positive trends are more concentrated in the southern part with some speckling to the north. The locations of the positive trends in September for q99 (Figure 5E) and q50 (Figure 5A) tend to be concentrated in the southern regions. Results indicate that increasing trends in precipitation are more widespread over the southeast and northeast, likely due to moisture coming in from the Gulf of Mexico. Further, the increasing trends seen in the warm season are probably coming mainly from July and September contributions.

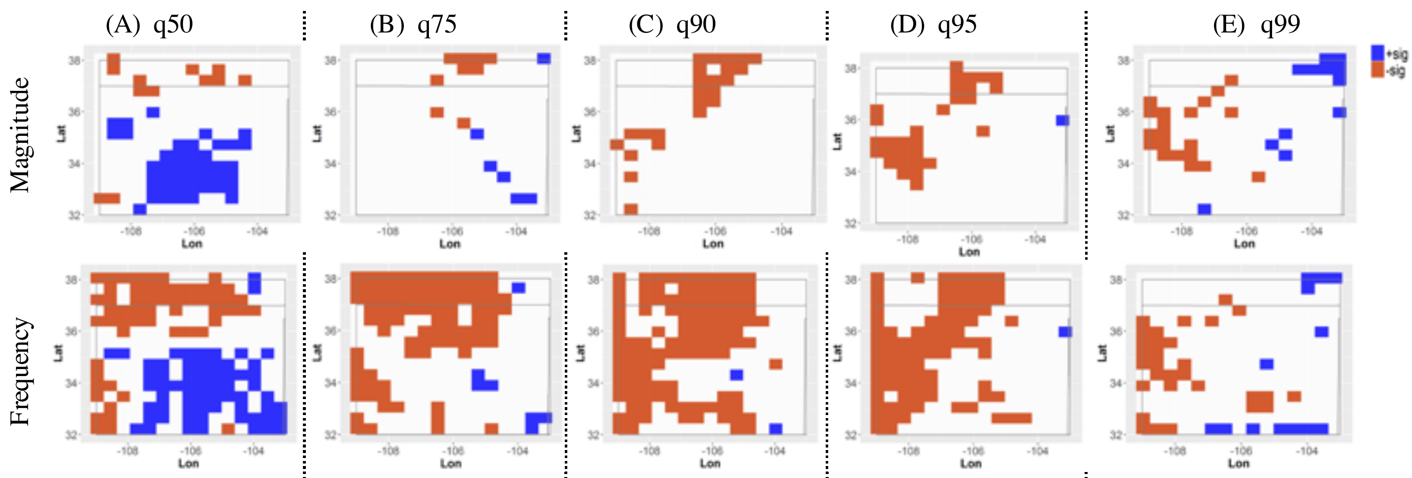

Figure 3. Spatial trend pattern in magnitude (top row) and frequency (bottom row) precipitation indicators for the warm season (June – October). The blue (red) areas indicate the location of the stations with increasing (decreasing) trends (p-values <0.05).

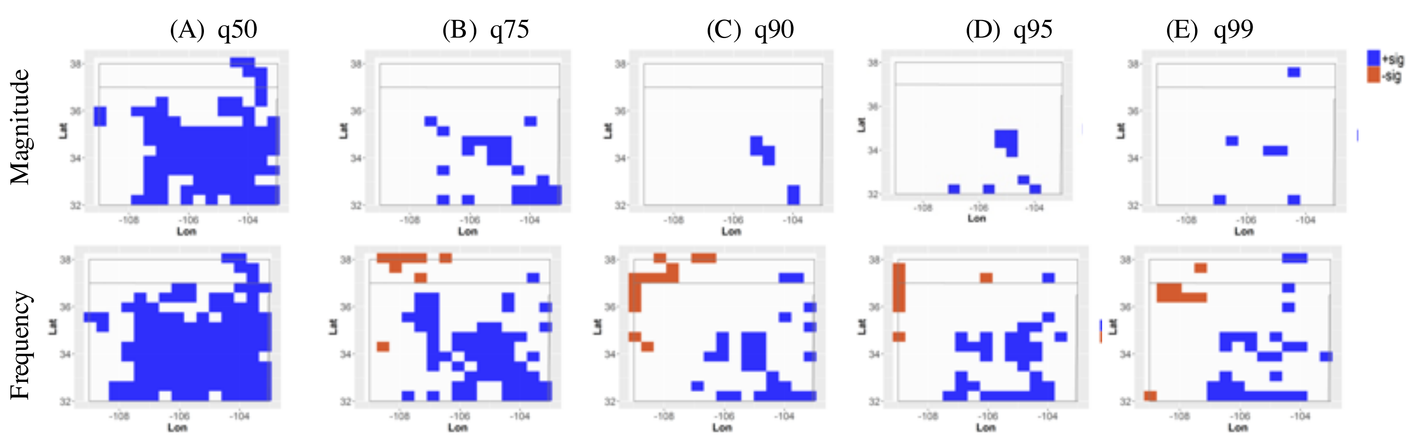

Figure 4. Spatial trend pattern in magnitude (top row) and frequency (bottom row) precipitation indicators for July. The blue (red) areas indicate the location of the stations with increasing (decreasing) trends (p-values <0.05).

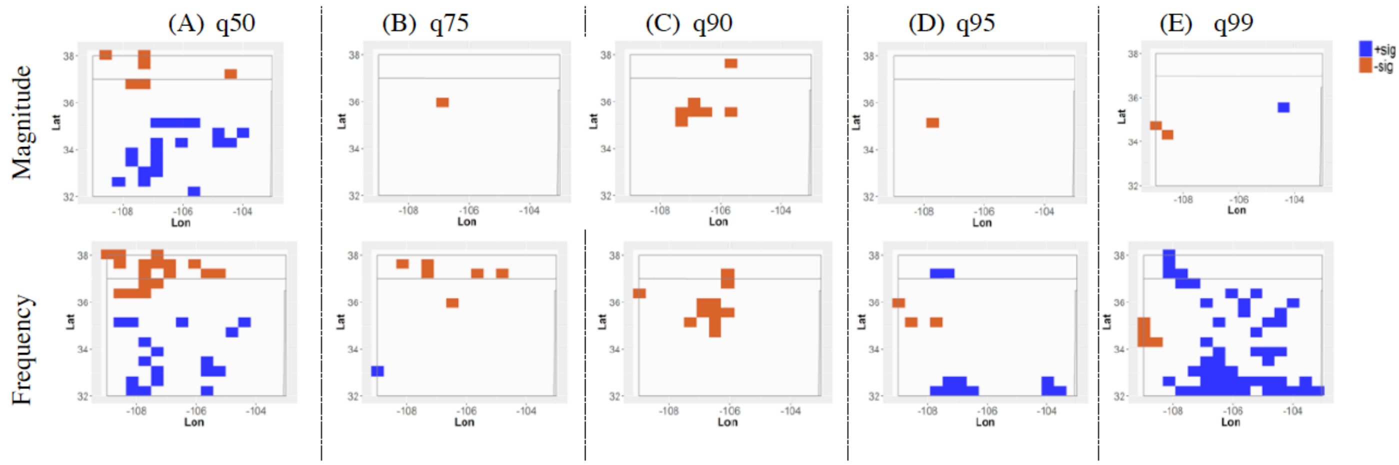

Figure 5. Spatial trend pattern in magnitude (top row) and frequency (bottom row) precipitation indicators for September. The blue (red) areas indicate the location of the stations with increasing (decreasing) trends (p-values <0.05).

Conclusions

In this study, we explore the trends in precipitation magnitude and frequency characteristics within the state of New Mexico and southern Colorado, relevant to the Rio Grande and Pecos basins. We examine both magnitude and frequency characteristics for the warm season (June - October) and individual months therein, with a focus on the upper quantiles and extremes. The purpose of this study is to determine how changing precipitation could potentially help mitigate decreases in water supply due to increasing temperatures and decreasing snowpack. For the period analyzed (1981-2017), we found that the dominant sign of the precipitation trend depends on the season/month examined. Negative trends dominate warm season, June, and August, while positive trends dominate July and for some September indicators, although the majority of locations in the study area did not show any significant trends. This suggests that the increasing trends across many of the July indicators show the most potential for water supply, with the location of these positive trends mainly concentrated in the southeastern and eastern part of the state. The frequency of days above q99 for September also showed increasing trends at some southern and southeastern locations, but this very heavy precipitation could be difficult to capture for water supply. However, across most characteristics examined, we find that significant trends are more detectable in the frequency indicators than the magnitude. For times and locations showing increasing trends, this suggests that water managers looking to exploit changes in precipitation might not need to plan for larger events, but rather more frequent events. Finally, we note that trend analysis provides important insight for water managers, especially in terms of where to focus further analysis. To this point, it is also critical to understand the drivers of the trends. In future work, the authors plan to investigate some of the factors that may be contributing to these trends, such as large-scale climate phenomena (e.g., the El Nino Southern Oscillation) or changes in the frequency of weather conditions (e.g., Prein *et al*., 2016).

Acknowledgements

This work was supported by the Bureau of Reclamation Science & Technology award No. 1782: “Detecting, Interpreting, and Modeling Hydrologic Extremes to Support Flexible Water Management and Planning.” This material is based upon work supported by the National Center for Atmospheric Research (NCAR), which is a major facility sponsored by the National Science Foundation (NSF) under Cooperative Agreement No. 1852977.

References

Asmerom, Y., Polyak, V. J., Rasmussen, J. B. T., Burns, S. J. & Lachniet, M. (2013) Multidecadal to multicentury scale collapses of Northern Hemisphere monsoons over the past millennium. *Proc. Natl. Acad. Sci.* **110**(24), 9651–9656.

Dobson, A. J. & Barnett, A. (2008) *An introduction to generalized linear models*.

Fox, J. (2015) *Applied regression analysis and generalized linear models*.

Gutzler, D. S. (2013) Climate and drought in New Mexico. In: *Water Policy in New Mexico*, 72–86.

Kendall, M. G. (1975) Rank Correlation Methods; Charles Griffin: London, 1975.

Llewellyn, D. & Vaddey, S. (2013) *West-Wide Climate Risk Assessment: Upper Rio Grande Impact Assessment: Report*. US Department of the Interior, Bureau of Reclamation, Upper Colorado Region, Albuquerque.

Mallakpour, I. & Villarini, G. (2017) Analysis of changes in the magnitude, frequency, and seasonality of heavy precipitation over the contiguous USA. *Theor. Appl. Climatol.* **130**(1–2), 345–363.

Mann, H. B. (1945) Non-Parametric Tests against Trend. Econmetrica, 13, 245-259.

Mote, P. W., Hamlet, A. F., Clark, M. P. & Lettenmaier, D. P. (2005) Declining mountain snowpack in western North America. *Bull. Am. Meteorol. Soc.* **86**(1), 39–49.

Pournasiri Poshtiri, M. & Pal, I. (2016) Patterns of hydrological drought indicators in major US River basins. *Clim. Change* **134**(4), 549–563.

Prein, A. F., Holland, G. J., Rasmussen, R. M., Clark, M. P. & Tye, M. R. (2016) Running dry: The US Southwest’s drift into a drier climate state. *Geophys. Res. Lett.* **43**(3), 1272–1279.

Serreze, M. C., Clark, M. P., Armstrong, R. L., McGinnis, D. A. & Pulwarty, R. S. (1999) Characteristics of the western United States snowpack from snowpack telemetry (SNOTEL) data. *Water Resour. Res.* **35**(7), 2145–2160.

Solomon, S., Qin, D., Manning, M., Averyt, K. & Marquis, M. (2007) *Climate change 2007-the physical science basis: Working group I contribution to the fourth assessment report of the IPCC*, Vol. 4. Cambridge university press.

Appendix B – Component 2 Paper Placeholder

The second component of the research project was to identify weather types (WTs). A manuscript containing pertinent data and results pertaining to this component has been finalized and submitted to a refereed journal. The principal investigator of this work will update this section to include the submitted manuscript once the journal peer review process has been resolved and information is ready for public dissemination. This is the placeholder for the manuscript. The abstract is included below:

The Changing Character of the North American Monsoon and its Impacts on New Mexico's Precipitation

By Andreas F. Prein, National Center for Atmospheric Research

Abstract:

The North American Monsoon (NAM) contributes up to 60 % to New Mexico's annual precipitation. With progressing climate change, monsoon precipitation will become even more important since spring and summer runoff from melting snowpack is decreasing with increasing warming. Here I identify four hydrologically important warm-season weather types (WTs) and aim to understand how their changes alternate New Mexico's precipitation. Observations show that New Mexico experienced a 15 % precipitation decrease between 1980 to 2010, which is caused by a shift towards more frequent dry WTs (-2 % per decade) and decreasing precipitation rates in two of the four WTs (-3 % per decade). Data from a regional and a global climate model ensemble show that the observed trends in WTs are likely caused by natural climate variability rather than anthropogenic climate change. However, future climate projections show a forced 5% decrease in monsoonal flow days until mid 21st century and a rapid increase thereafter resulting in 15% more monsoonal flow days at the end of the century compared to 1990–2019. The processes that trigger these nonlinear changes are unclear but they are caused by increasing greenhouse gas forcing rather than changes in aerosols or land use. How this will affect New Mexico's warm-season precipitation is uncertain. All models overpredict precipitation on dry WT days by more than 100%, which reduces the future wetting that should result from more frequent monsoonal flow days. Changes in precipitation rates strongly depend on the global climate model but higher resolution regional models increase future precipitation rates compared to their coarse-resolution counterparts.

Appendix C – Component 3 Paper

Extreme-value analysis for the characterization of extremes in water resources: A generalized workflow and case study on New Mexico monsoon precipitation

Erin Towler[1], Dagmar Llewellyn[2], Andreas Prein[1], Eric Gilleland[1]

[1] National Center for Atmospheric Research, Boulder CO

[2] U.S. Department of Interior, Bureau of Reclamation, Albuquerque, NM (Opinions expressed represent professional opinions of the co-author, not official positions of the government)

Paper accepted for publication in Weather and Climate Extremes

Abstract

Water managers need non-stationary tools to better characterize precipitation extremes. Statistical approaches based on extreme value theory (EVT) are increasingly being used, but few end-to-end generalized workflows are available. In this paper, a step-by-step framework is demonstrated for developing an EVT model that considers the influence of dominant weather patterns on precipitation extremes in a watershed. Specifically, the Point Process (PP) model is utilized, which is a unified statistical framework for modeling the frequency and magnitude of extremes above a threshold. Because threshold selection can be subjective, a demonstration of how to go about selecting a threshold is provided; in particular, by examining a range of thresholds. The workflow is applied to daily precipitation from the Rio Grande watershed in New Mexico. In this arid watershed, extreme precipitation events substantially contribute to total runoff. An improved understanding of the drivers and extent of changes in extreme precipitation is essential for water resource and risk management. In addition to a stationary PP model without covariates, several covariates are examined for inclusion in the location and scale parameters. The significance of including the covariates is assessed, as well as several additional criteria, including if the covariate(s) make intuitive sense and if it is a good candidate for statistical downscaling (i.e., methods that relate large-scale variables to the local scale). A final PP model is selected that includes the wet weather types in the location and scale parameters. This model is applied in a downscaling context using a large ensemble of climate projections, which shows that the frequency of exceeding a high threshold increases after 2050, but the conditional likelihood of exceeding the maximum observed precipitation stays relatively constant.

1. Introduction

Precipitation extremes are of particular importance to water resources, because of both the management threats, such as flooding, and potential opportunities, such as water supply, that they provide. Given climate variability and change, water managers need non-stationary tools that can better characterize precipitation extremes, and changes in patterns of extreme precipitation over time. Dynamical modeling tools such as the Weather Research and

Forecasting (WRF) model (Skamarock et al. 2005, Powers et al. 2017) with kilometer-scale horizontal grid spacing have been used to examine heavy precipitation (e.g., Mahoney et al. 2013; Prein et al. 2013). However, high-resolution dynamical downscaling requires considerable expertise and computational power. Statistical approaches can be complementary to these dynamical models, as they are computationally inexpensive, and are quite flexible so that they can easily be transferred across applications and regions (Fowler et al. 2007).

Extreme Value Theory (EVT, Coles 2001) is a statistical framework to evaluate and simulate the extremes of a distribution, and is well suited to the disciplines of hydrology and water management (Katz et al. 2002). Extremes in a dataset are typically examined in two ways: either using the block maxima approach, where the maximum values for a given time block are extracted from the time series, or the peaks-over-threshold (POT) approach, which analyses extremes that exceed a high threshold. The generalized extreme value (GEV) distribution is appropriate for fitting to block maxima data, and the approach has been applied widely in water resources. However, this approach has the disadvantage of ignoring multiple extremes that may have occurred during a given time block. The POT approach overcomes this limitation and allows for the analysis of all independent extremes data by fitting the generalized Pareto (GP) distribution. The point process (PP) model allows for inferring about the frequency and magnitude of values above a threshold.

An advantage of EVT is that it is possible to account for non-stationarity; that is, its techniques can include predictors or covariates to vary the likelihood of the extremes. This approach can be useful for water managers to characterize their changing risk profiles, for instance, the shifting likelihood of an extreme based upon changing land surface or meteorological conditions. In this context, EVT can be applied as a form of statistical downscaling (Katz 2002). Statistical downscaling is a general term that refers to a range of methods that relate large-scale climate variables to local or regional variables. Maraun et al. (2010) provide a comprehensive overview of methods for downscaling precipitation under climate change, though most downscaling techniques have not been developed to target extreme precipitation, with EVT as the notable exception. Recent work has compared the skill of commonly used statistical downscaling techniques for water resources, not including EVT, which shows that most of the approaches do have some skill at estimating extremes, although the skill varies between techniques, and deficiencies remain (Gutmann et al. 2014).

A multitude of software packages have made EVT accessible to more users (Gilleland et al. 2013b) and detailed illustrative examples of how to apply software packages to diverse datasets are available (Gilleland and Katz 2016). This paper continues in this vein, providing a generalized workflow for applying EVT to precipitation extremes in a water resources context. Specifically, a PP model is developed and demonstrated that includes the influence of different weather types on the precipitation extremes in a watershed. Developing a PP model is a more complex EVT modeling approach, first because it is a POT approach that requires threshold selection and extremal independence, and second because it provides information about both the frequency and magnitude of extremes, which requires additional interpretation. Incorporating covariates to account for non-stationarity also adds complexity. However, these features also make the PP a powerful approach, and our aim is to help users to think through its implementation in a systematic way.

2. Statistical Methods: The Point Process (PP) Model

In this paper, the PP characterization of extreme-value analysis (EVA) is adopted. The PP model allows for making inferences about both the frequency and intensity of extreme values. Following from Gilleland and Katz (2016), the non-homogeneous Poisson point process with intensity measure, Λ, on the set $A = (t_1, t_2) \times (x, \infty)$ is given by:

$$\Lambda(A) = (t_2 - t_1) \cdot \left[1 + \xi \frac{x - \mu}{\sigma}\right]^{-1/\xi} \cdot I(1 + \xi \cdot (x - \mu)/\sigma \geq 0)$$

where $-\infty < \mu, \xi < \infty$ and $\sigma > 0$ are location, shape and scale parameters, respectively, $I(\cdot)$ is an indicator function that is zero if the argument is not true and one otherwise. Substituting $[t_1, t_2]$ $=[0,1]$ to represent one year (or season), and if the indicator function is 1, the Poisson rate parameter, λ, can be calculated to obtain the frequency of exceeding a particular threshold, u:

$$\lambda = \left[1 + \xi \frac{u - \mu}{\sigma}\right]^{-1/\xi}$$

To estimate the parameters of the PP model, maximum likelihood estimation (MLE) is used here; for a high threshold, u, the PP log-likelihood, ℓ, is estimated as:

$$\ell(\mu, \sigma, \xi; x_1 \ldots x_n) =$$

$$-k \ln \sigma - \left(\frac{1}{\xi} + 1\right) \sum_{i=1}^{n} \left[1 + \frac{\xi}{\sigma}(x_i - u)\right]_{x_i > u} - n_y \left(1 + \frac{\xi}{\sigma}(u - \mu)\right)^{\frac{-1}{\xi}},$$

Where n_y indicates the number of years of data and $[\cdot]_{x_i > u}$ is the indicator function (as in equation 10 in Gilleland and Katz 2016). It is also possible to fit the generalized Pareto (GP) distribution to just the threshold excesses; estimating the frequency separately. This approach is called the orthogonal approach, and while it is better to fit the entire PP model to the data so that all of the uncertainty in estimating these parameters is simultaneously accounted for, it is easier to fit the GP distribution to data, so it is used later in this paper to help inform the estimation of the PP model.

The parameters can vary with covariates, or predictors, to account for non-stationarity. For example, the location parameter could be modeled as a linear function of a covariate, x:

$$\mu(x) = \mu_0 + \mu_1 x\ ,$$

And similarly, the scale parameter can also be modeled with a covariate. Because the scale parameter must be positive everywhere, it is often modeled with a log-link function:

$$\ln \sigma(x) = \phi_0 + \phi_1 x$$

It is also possible to add a covariate to the shape parameter, but given that the shape parameter estimates have large confidence intervals, it is assumed to be constant in time. Further, different functions (quadratic, nonlinear), or multiple covariates could be investigated. Here, the inquiry is limited to linear functions for simplicity.

To test covariate significance, a likelihood-ratio test is used. From Coles 2001 (section 2.6.6), if a model M_0 is a sub-(i.e., nested) model of M_1, the deviance statistic, D, can be calculated from the maximized log-likelihoods for the models:

$$D = 2[\ell_1(M_1) - \ell_0(M_0)]$$

If $D > c_\alpha$, then M_0 can be rejected for M_1, where c_α is the $(1-\alpha)$ quantile of the χ_k^2 distribution. The level of significance is α, and the χ_k^2 distribution is the large sample approximation with degrees of freedom, k. Results from the likelihood-ratio test are shown as p-values, and tested using $\alpha = 0.05$ and $\alpha = 0.10$. Models are also compared based on the Akaike Information Criterion (AIC) [Akaike, 1974], which can be calculated as:

$$AIC = -2(\ell) + 2K$$

Where ℓ is the likelihood function estimate, and K is the number of parameters being estimated.

3. Workflow Methodology

This section provides the generalized workflow for fitting a non-stationary PP model to extreme precipitation in a water management context. Figure 1 shows the generalized workflow, which provides the outline for the below sections. All analyses are performed in the open-source R (R Core Team 2019) extRemes package (Gilleland and Katz 2016). In Gilleland and Katz (2016), functions for several diverse analyses are applied to different types of datasets. However, it does not follow an end-to-end workflow. Part of our contribution is to outline a step-by-step process that can provide guidance for estimating and interpreting the non-stationary PP model for water management and planning.

3.1 Extract Independent Peaks over Threshold

The first step towards developing a PP statistical model is to extract the extremes that will be fitted. As mentioned, to maximize the amount of data, a POT approach is adopted, which requires selecting a threshold. Selecting a threshold represents a tradeoff between minimizing bias and variance: if the threshold is too low, it will violate the statistical assumptions of EVT, leading to high bias, but if the threshold is too high, there will not be enough data remaining to effectively estimate the parameters, leading to high variance (Coles 2001). Several threshold selection diagnostic plots can aid in the selection, including the mean residual life plot and examining the model parameters across a range of thresholds (Coles 2001, and see Gilleland and Katz 2016 for extRemes commands). However, it is important to note that there is some subjectivity to threshold selection, and that several thresholds (or a range of thresholds) may be reasonable. As such, in this workflow a range of thresholds are examined.

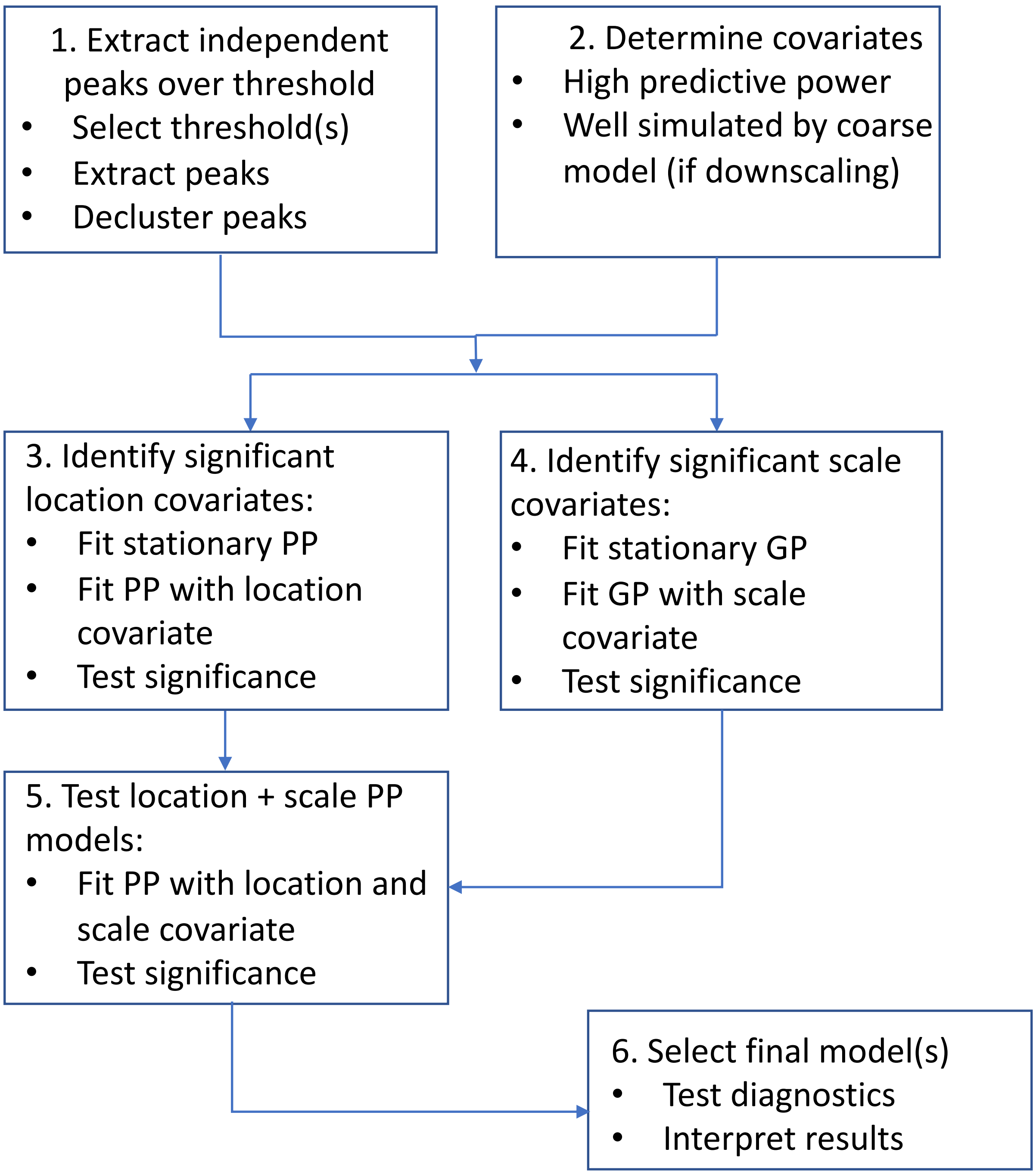

Figure 1. Flow chart for fitting the Point Process (PP) model.

Further, to produce realistic estimates of the uncertainty in estimating parameters and return levels, it is prudent to test the extreme data for independence, and make modifications to try to obtain independence if they are not. In water resources applications, which often involve meteorological data (e.g., precipitation), time series are often autocorrelated. As such, the data need to be tested for dependence, and declustered if necessary. Coles (2001) outlines ways to diagnose the dependence, for instance using visual inspection, such as the auto-tail dependence function plot (atdf, Reiss and Thomas 2007), and the extremal index. The extremal index ranges between 0 and 1, with values closer to 1 indicating less dependence. Coles (2001) also discusses methods for declustering, which can be implemented readily in extRemes (see Gilleland and Katz 2016). In this workflow, examining the effect of declustering using the extremal index is recommended.

3.2. Determine covariates

A key to using EVT in a downscaling context is to identify appropriate covariates. Maraun et al. 2010 summarize the key criteria, including that predictors must have high predictive power or explanatory power. It is important to note that covariate selection is to some extent subjective, and results are dependent upon predictor selection (Fowler et al. 2007). In a climate-change context, it is critical that the covariate is well-represented by the coarse-resolution dynamical model, and that the predictive relationship is thought to be constant, i.e., it does not change over time (Wilby et al. 2004). Simulating precipitation extremes directly is challenging because the physical processes responsible for them occur on very small scales (Seneviratne et al. 2012). However, climate models are able to skillfully reproduce large-scale circulation patterns (Flato et al. 2013), which can be an appealing covariate option. One popular approach in the downscaling literature has been to identify so-called “weather types”, which are recurring large-scale atmospheric patterns that are associated with precipitation (Maraun et al. 2010; Wilby et al. 2004). In terms of water resources applications, this is a departure from the status quo, since most impact studies to date essentially use precipitation as a covariate; that is, precipitation is downscaled from coarser scales to finer scales (Guttman et al. 2014). However, this could be problematic given the uncertainty in simulating precipitation from climate models (Collins et al. 2013), especially when it comes to extremes.

3.3 Identify significant location parameter covariates

The next step is to identify which, if any, location covariates improve the fit, and for what thresholds. For each threshold, the stationary PP model is fit to the data, i.e., without covariates, as well as the non-stationary PP model, i.e., where each covariate is tested for whether or not it is reasonable to include it as part of the model for the location parameter. The likelihood-ratio test is employed here to assess if including the location covariate is significant. This process is repeated for each threshold and each covariate.

3.4. Identify significant scale parameter covariates

The scale parameter affects the spread of the distribution. In this step, the significance of the scale covariate using the GP model is tested. Within the PP modeling framework, it is not necessary to explicitly fit the GP to the threshold excesses, rather the likelihood function for the PP can be maximized directly to estimate the parameters. However, the purpose of this step is to identify potential scale covariate candidates before developing the full PP model (i.e., in upcoming section 3.5). Hence, when looping through many covariates and thresholds, it is simpler to implement and interpret the GP model fit. As such, the stationary GP model and non-stationary GP model are fit to the threshold excesses by incorporating the scale covariate, and the likelihood-ratio test is used to assist in determining whether or not to include them in the final PP model. This procedure is repeated for each threshold and covariate.

3.5. Test location and scale PP models

The next step is to test the significance of a PP model that includes non-stationarity in the location and scale. Here, outputs from the previous two steps (3.3 and 3.4) can be used to inform what location and scale model combinations should be tested. From Section 3.3, only models with thresholds where the location parameter covariate is significant are tested further. Output from Section 3.4 is used as a diagnostic to identify which scale covariates should be tested with the location covariates from Section 3.3. The non-stationary PP model with a location covariate and a non-stationary PP model with a location and scale covariate are fit to the data, and the likelihood-ratio test and AIC values are used to help evaluate their importance in the model. The result is helpful at informing if including both the location and scale covariate in the model is significant for that threshold.

3.6. Select final model(s)

The final step is to examine the output from the prior step, and to select the final model(s). There is some subjectivity to this step, but it includes examining fit diagnostics, such as the quantile-quantile plots (qqplots), which are readily created in extRemes (Gilleland and Katz 2016), as well as the AIC values. It is also important, here, to investigate whether or not the covariates are physically meaningful, as well as if they are suitable for downscaling, and to determine if they have utility for water management.

4. Case Study Overview

The Rio Grande watershed in New Mexico (NM) is used to demonstrate the generalized workflow. Similar to many water systems in the western United States, one key vulnerability for the Rio Grande is decreasing snowpack (Chavarria and Gutzler 2018), which has historically been the primary water source for NM. As such, water managers have a renewed interest in their secondary water source: warm-season precipitation. In summer, the central and southern parts of New Mexico are influenced by the North American Monsoon (Gutzler 2013; Adams and Comrie 1997), which result in significant contributions to annual precipitation (Douglas et al. 1993). Towler et al. (2019) show that although monsoon season streamflow volumes vary from year-to-year, they are an important contribution to annual water supply in NM. Further, most extreme precipitation in NM (Kunkel et al. 1999) as well as most observed flooding (Villarini 2016), occurs in summer. Therefore, there is an interest in understanding the predictability of warm-season precipitation characteristics, including extremes. Extremes are often considered for flood risk, but have been less explored in terms of potential opportunities for water supply, which is the primary interest here. From a water management perspective, extreme precipitation events from summer monsoon or remnant hurricanes are relevant for both operational planning, such as optimizing reservoir management, as well as for assessing the need for more temporary detention of water in downstream reaches, including within irrigation networks, so that water from an extreme event can be used over time, rather than simply flushed downstream. In this study, the focus is restricted to the monsoon season - July, August, and September - and remnant hurricanes are not explicitly considered, which tend to provide occasional high contributions during the otherwise relatively dry month of October (Wood and Ritchie 2013).

Daily precipitation data from PRISM Gridded Climate Data Group (prism.oregonstate.edu), downloadable from http://www.prism.oregonstate.edu/documents/PRISM_downloads_FTP.pdf are used. All of the points within the Rio Grande watershed upstream of the Elephant Butte Reservoir, a large- reservoir in south-central NM (Figure 2) are taken as a subset. The Rio Grande watershed extends into southern Colorado, but this region is excluded because it is the headwater of the basin, where most of the current water storage already exists to capture snowmelt runoff, and interest is centered on warm season moisture that occurs in, and could potentially be captured in, NM. Because of the interest for water supply, it is the extreme values across the watershed that are of primary interest, so the daily precipitation are spatially averaged. For assessing local risk, it is not a good idea to first average data before looking at extremes. However, accounting for spatial dependence in the extreme values is a challenging task that is computationally very intensive. Therefore, utilizing a spatial average allows for gleaning a picture of extremes in a climatological sense over the entire region. The daily spatial averages in each year's monsoon season July-September are investigated, resulting in 92 days per year. Data are available from 1981-2018 (38 monsoon seasons). Figure 2 shows how most of the differences in precipitation climatology (Figure 2b) are related to orography (Figure 2a). An alternative to taking the spatial average that would be more conservative would be to take the spatial maximum; this would be more appropriate if the primary interest was in flood risk, rather than potential opportunities for water supply, which is the primary interest here.

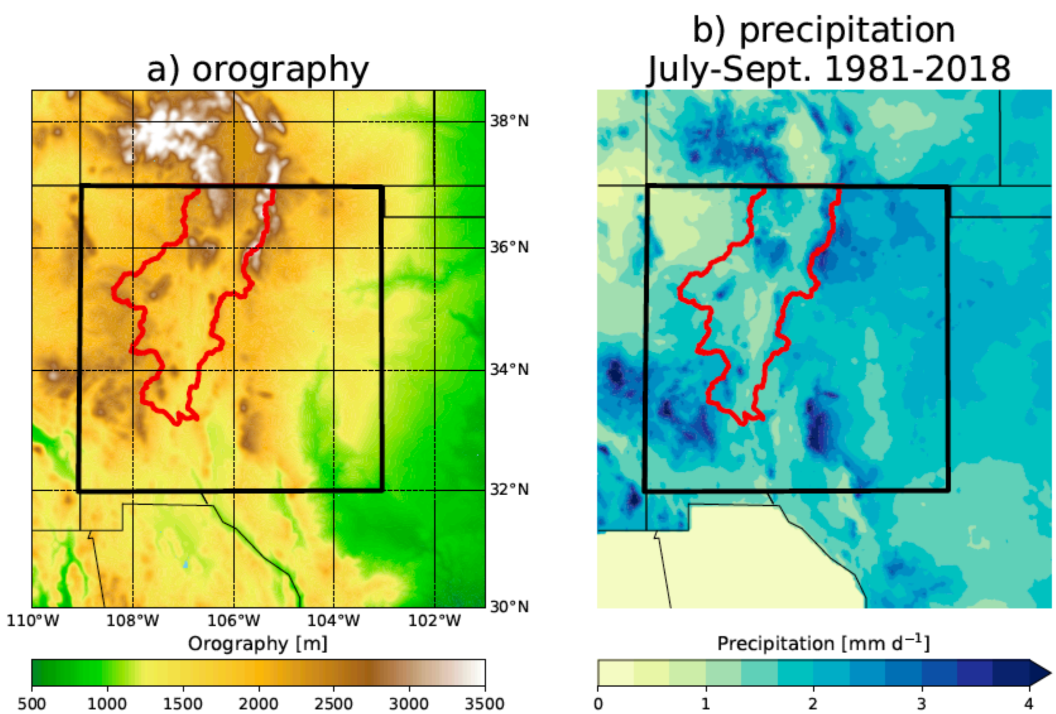

Figure 2. Rio Grande watershed above Elephant Butte Reservoir (red outline) in New Mexico (bold black line) showing a) orography and b) average daily precipitation for the monsoon season (July-September) from 1981-2018.

5. Results

In this section, the results for each step of the workflow are demonstrated, as applied to the NM Rio Grande watershed.

5.1. Extracting the Independent POT

The first step is to extract the POT data, which in this case come from the daily monsoon precipitation data described in Section 4. Figure 3 shows the daily precipitation for each year's monsoon season over the NM Rio Grande watershed. Horizontal lines show several quantiles: Q91 is 5.0 mm, Q95 is 7.0 mm, and Q99 is 11.9 mm. The maximum value (Q100) is 25.7mm. For threshold selection, the PP model is fit to data across a range of thresholds and how the fitted parameters vary is checked (Supplemental Figure 1). For all three of the parameter estimates, these quantile values, including the uncertainty bounds, do not change much using thresholds from 4mm to 12mm, though it starts to change after 13mm. This result is backed up by the qqplots, which show 4mm to be a reasonable choice, while the qqplot is less straight for 13mm (Supplemental Figure 2); this degrade in fit diagnostic is to be expected as the sample size decreases. Although it is desired to pick a lower value to maximize the sample size, the exact threshold value to select is somewhat subjective. For this study, the Q91(=5.0 mm) is selected as a minimum, so the range of thresholds from 5 mm to 12 mm by 0.5 mm increments are examined.

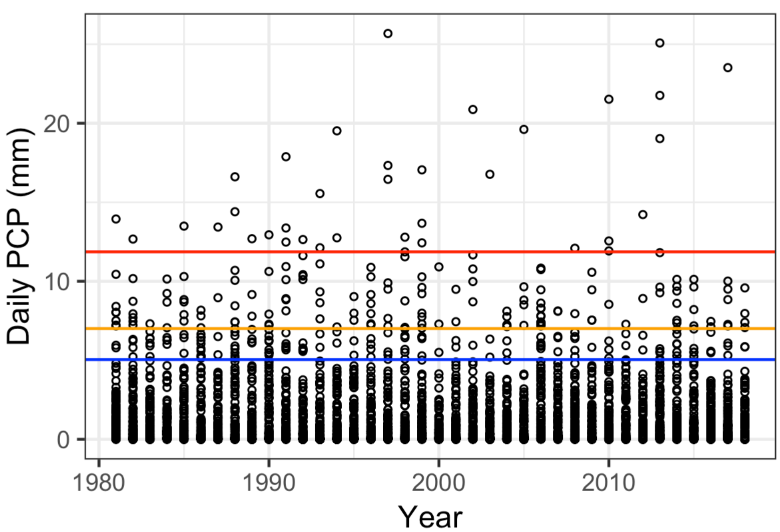

Figure 3. Monsoon (July-September) daily precipitation averaged over the New Mexico Rio Grande watershed from 1981-2018. Horizontal lines are select quantiles: Q91=5.0mm (blue), Q95=7.0mm (orange), and Q99=11.9 mm (red).

While not important for estimating the parameters themselves, the estimated uncertainty will be too low if the data above the threshold are not independent. Because daily precipitation data are often highly autocorrelated, it is prudent to test for dependence. As expected, visual inspection using the auto-tail dependence function plot (atdf) showed that there is some dependence in the tails (see Supplemental Figure 3) and that the dependence should be accounted for in the analysis. The extremal index is also examined, which is a more automated approach for testing the effect of declustering. Using the runs method for declustering (see Coles, 2001 sec. 5.3.2), implemented in the extRemes package, the extremal index is calculated for the raw and declustered data. For every threshold tested below 12mm, the extremal index increases/improves (the extremal index for the 12mm threshold stays constant at 1; see Supplemental Table 1). Further, the PP stationary model is fitted with the original and declustered data, and compared using the AIC; the result showed that the declustered data resulted in lower AIC (better fit) for every threshold despite reducing the data retained (see Supplemental Table 1). Hence, all subsequent results use the declustered POT data.

5.2. Determining the Covariates

As mentioned in Section 3.2, it is important to select covariates based on their predictive and explanatory power, as well as how well they are represented in climate models. One appealing option that has gained credibility in climate-change studies is to use large-scale circulation patterns (Christensen et al. 2013). This approach is particularly attractive in regions and seasons, such as NM during mid- to late-summer, where large-scale climate oscillations, such as the El Niño–Southern Oscillation, provide limited opportunities for improving weather predictability (Vigaut et al. 2017). In a companion study, Prein (2019) identifies four hydrologically important weather types that occur during NM’s warm season. The algorithm is identical to Prein et al. 2016 and 2019 and maximizes the skill of differentiating precipitation anomalies and extreme precipitation events over NM by iterating over four different domain sizes focused on NM, seven input variables, and the number of weather types. Aiming for a small number of weather types, optimal performance is found for selecting four weather types over a domain covering NM and using three large-scale input variables – precipitable water, sea level pressure, and low-level (850 hPa) wind speed. The data is based on instantaneous values at 12:00 UTC (Universal Time Coordinated). These variables relate to both dynamic and thermodynamic processes associated with precipitation. A domain the size of NM was selected. Figure 4 shows the four identified circulation patterns and precipitation anomalies for the weather types (WTs). WT1 and WT2 are associated with dry conditions, and WT3 and WT4 are associated with wetter conditions.

The frequency of days within a weather type are related to extreme precipitation since extremes are very unequally distributed between the four weather types (see Figure 5). Figure 5a shows that the four weather types have a similar amount of days in each warm season climatologically. However, the average contribution to NM's warm season mean rainfall and heavy precipitation events are very unequally distributed with WT4 contributing ~50 % of the warm season rainfall (Figure 5b) and 60% of all heavy events occurred in this weather type (Figure 5c). WT3 has lower (but positive) precipitation anomalies, and less intense precipitation than WT4.

To obtain the covariates, the number of days in each weather type for the warm season are summed, and then this becomes the (seasonal) covariate upon which the (daily) precipitation data are conditioned. The average of each large-scale variable (i.e., precipitable water, sea level pressure, and wind speed) as a covariate is also explored; average values are calculated by 1) averaging the daily values over each year’s monsoon season, and 2) spatially averaging over the entire state of NM. The gridded large-scale data were from ECMWF’s Interim Reanalysis (Dee et al. 2011) (ERA-Interim); see Prein (2019) for details. Table 1 shows the covariates examined. Year was also examined as a covariate to see if there was a temporal trend to the extreme values.

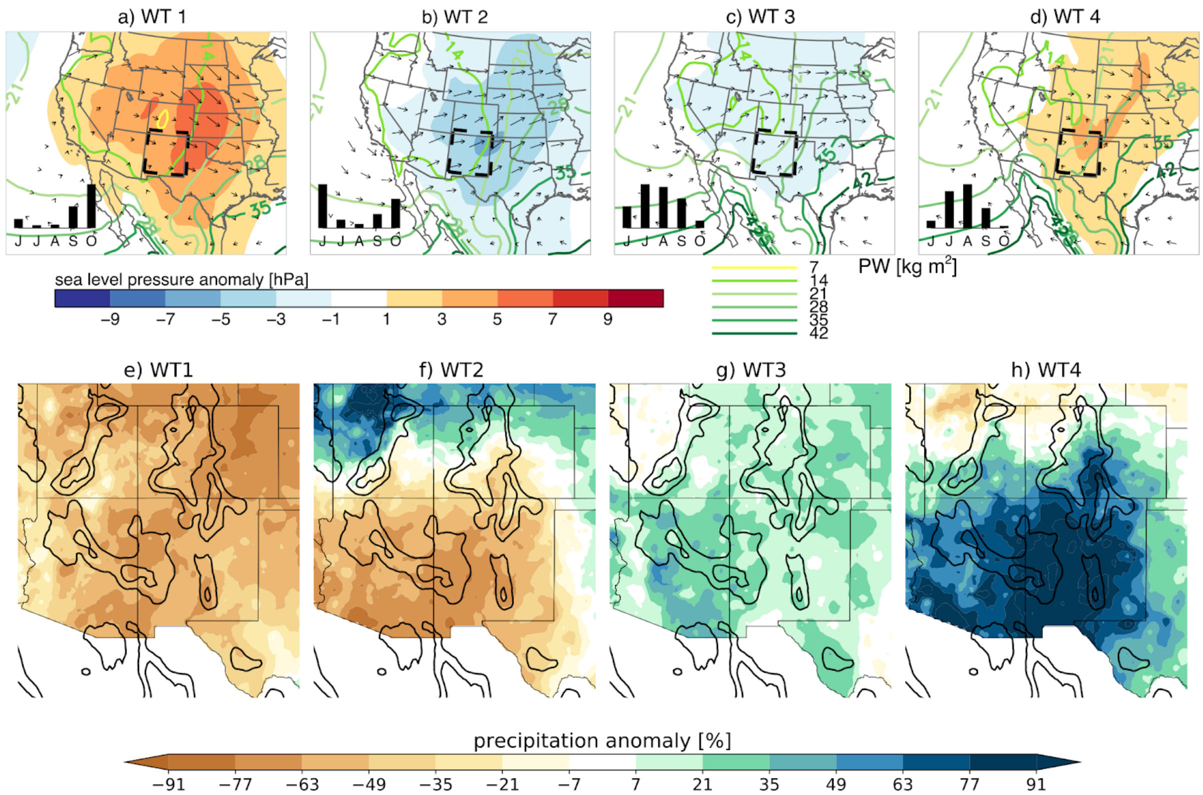

Figure 4. Circulation patterns based on sea level pressure, precipitable water (PW), and 850-hPa wind speed and direction (arrow length and angle) for Weather Types (WT) 1 – 4 (a-d). The data is based on instantaneous values at 12:00 UTC. Note that only the wind speed component was used in the weather typing. Associated daily precipitation anomalies are shown in (e-h).

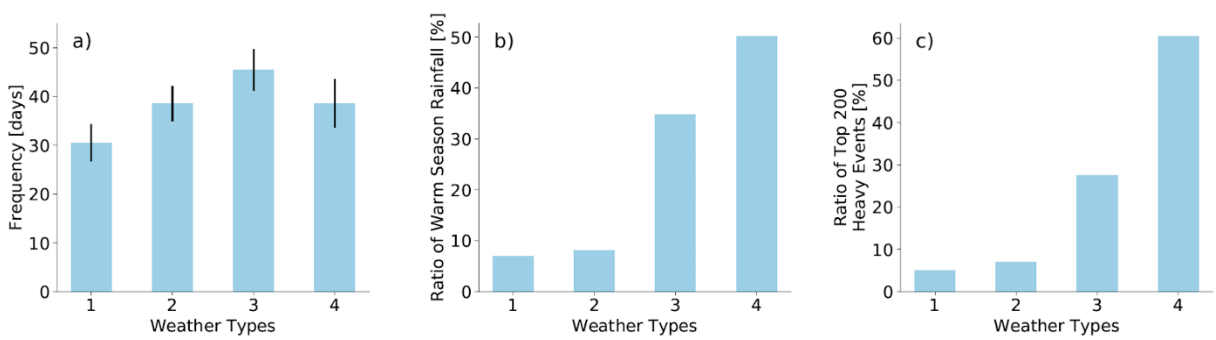

Figure 5 (a) Climatological average (1979 to 2014) frequency of weather types (WTs) between June to October; (b) WT contribution to total precipitation over New Mexico; (c) the number of the top 200 heaviest precipitation events associated to the WT under which they occur.

5.3. Identifying Significant Location Covariates

For each threshold, the stationary PP model (no covariates) is fit to declustered POT data. A non-stationary PP model is also fit using each of the covariates in Table 1 as linear predictors in the location parameter. Figure 6 shows the likelihood-ratio test results for all the covariates tested, across thresholds. The results show that the fitting of the extreme-value data can be highly sensitive to the inclusion/exclusion of certain points: for instance, using Year as a covariate for a threshold of 6mm shows significance ($p<0.10$), but this result is not found for the other thresholds. Similarly, for the sum of WT4 over the season, if we had arbitrarily selected 7.5mm as a threshold, it would show non-significance ($p>0.10$), although the model is significant for thresholds less than 7.5 mm and greater than 7.5 up to 8.5 mm. This behavior is an important reminder that while the p-values can be used diagnostically to assess which covariates are reasonable to include, a statistical test should only be used as evidence to help guide scientific research and never employed in its stead.

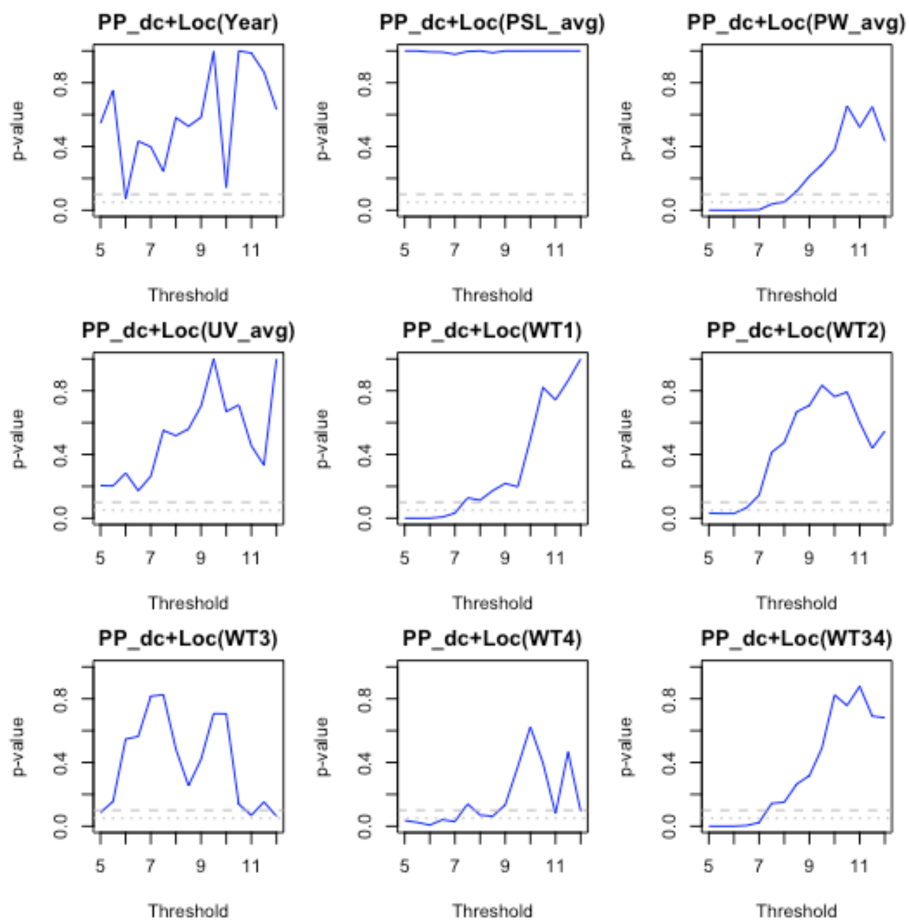

Figure 6. p-values from likelihood ratio test for declustered PP model (PP_dc) fit with location covariate (see title) over a range of thresholds. Horizontal lines are p=0.10 (dashed) and p=0.05 (dotted).

Figure 6 provides evidence for not including Year, average sea level pressure (PSL_avg), average wind speed (UV_avg), nor the sum of WT3 over the season as covariates in the location parameter, since they don't show much or any significance across the thresholds tested. On the other hand, the p-value results suggest that average precipitable water (PW_avg) and the sum of WT1, WT2, and WT4, as well as WT34 (i.e., the sum of WT3 and WT4 days) are all generally significant for the lower thresholds. This provides guidance to further constrain the upper bound for the thresholds examined in the next step to 8.5mm (rather than up to 12mm).

5.4. Identifying Significant Scale Covariates

Using the new threshold range (i.e., from 5mm to 8.5mm), the stationary GP model (no covariates) is fit to declustered threshold excess data. The GP distribution is also fit to the excesses using the covariates in Table 1 as linear predictors in the scale parameter. Figure 7 shows results for covariates that showed significance. The sum of WT3 is significant across most thresholds ($p<0.05$), which suggests that it would be a good scale covariate to test in the full PP model (next step). The sum of WT1 and WT34 are also shown to be significant for the lower thresholds, warranting further investigation.

Table 1. Variables considered for location and scale covariates.

Variable	Description
Year	Year of season
PW_avg	Average precipitable water over New Mexico for the season (kg m^2)
PSL_avg	Average sea level pressure over NM for the season (hPa)
UV_avg	Average wind speed over NM for the season (m/s)
WT1	Sum of weather type 1 days over the season
WT2	Sum of weather type 2 days over the season
WT3	Sum of weather type 3 days over the season
WT4	Sum of weather type 4 days over the season
WT34	Sum of weather type 3 and 4 days over the season

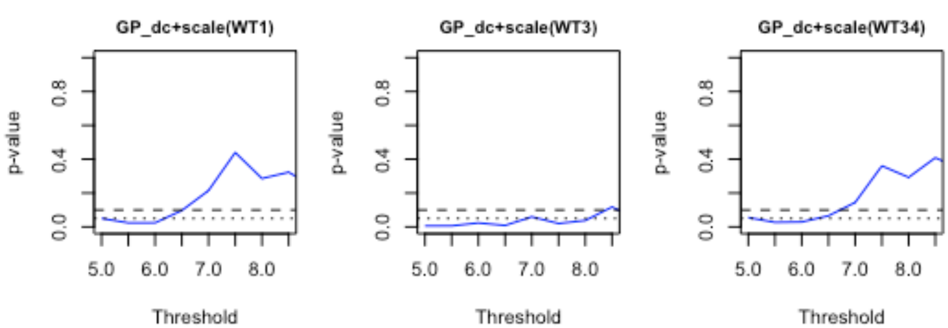

Figure 7. p-values from likelihood ratio test for declustered GP model (GP.dc) fit with scale covariate (see title) over a range of thresholds. Horizontal lines are p=.10 (dashed) and p=0.05 (dotted).

5.5. Testing the Location and Scale PP Models

Using the full PP, the location and scale combinations that are informed by the prior steps are tested. For the location parameter, PW_avg, WT4, WT1, WT2, and WT34 are tested for inclusion. For the scale parameter, WT3, WT1, and WT34 are tested. Table 2 shows results from the PP model with location covariates WT4 and PW_avg fit to the data, because those choices resulted in the lowest AIC values by threshold in the PP model. All model combinations tested and associated AIC values are shown in Supplemental Table 2. For the PP model with WT4 in the location, PP_dc+Loc(WT4), it is found that all three scale combinations result in improved fits according to both the likelihood-ratio test and the AIC. Results for using the location of WT1, WT34, and WT2 with the different scale parameters are shown in Supplemental Table 3; these models did not yield as many significant combinations and higher (worse) AIC values.

Table 2. p-values from likelihood ratio test for PP models for different combinations of location and scale. Bold indicates p-value <=0.05; red indicates lowest AIC by threshold.

Threshold (mm)	PP_dc+Loc(WT4)				PP_dc+Loc(PW_avg)			
	-	+sca(WT3)	+sca(WT1)	+sca(WT34)	-	+sca(WT3)	+sca(WT1)	+sca(WT34)
5	**0.04**	**0**	**0**	**0**	**0**	**0.01**	**0**	**0**
5.5	**0.02**	**0**	**0**	**0**	**0**	**0.02**	**0.01**	**0.01**
6	**0.01**	**0**	**0**	**0**	**0**	0.12	0.13	**0.04**
6.5	**0.04**	**0**	**0.03**	**0.01**	**0**	0.08	0.38	0.09
7	**0.03**	**0.04**	0.23	0.11	**0**	0.44	0.93	0.43
7.5	0.14	**0.03**	0.39	0.28	**0.04**	0.22	0.92	0.60
8	0.07	0.08	0.36	0.27	**0.05**	0.41	0.6	0.42
8.5	0.06	0.26	0.47	0.47	0.12	0.78	0.57	0.57

5.6. Selecting Final Model(s)

The last step is to select the final model(s), which has an element of subjectivity. Here, several additional criteria are considered: 1) the parameter is a good candidate for downscaling, and 2) the covariate(s) make intuitive sense. PW_avg makes intuitive sense, but is not ideal to use it directly in our downscaling: although PW_avg is projected to increase because of warming (e.g., Soden and Held 2006), it only represents a thermodynamic response, and ignores the dynamical response (e.g., changes in circulation). In short, it may be too simple to assume it is the only factor that would influence extremes. WT4 makes physical sense because it is one of the wet weather types that tends to be associated with heavy precipitation. Further, the WTs are based on variables (i.e., precipitable water, sea level pressure, and wind) that represent both thermodynamic and dynamic properties associated with precipitation.

As mentioned previously, it was found that the PP_dc+Loc(WT4) model has improved fits using all three scale combinations, at least for some of the thresholds. Here, again, there needs to be scientific reasoning, as well as some subjectivity, that contribute to the selection of what, if any, scale covariate should go into a final model. Because WT34 combines the sum of days for the two wet WTs, it is more difficult to interpret, so it is not selected here. WT1 and WT3 both have inverse relationships with WT4 (Supplemental Figure 4), so it is consistent that both of these covariates are identified as significant additions to the model. One thing to notice is that incorporating WT3 in the scale improves the fit for most of the thresholds, whereas WT1 and WT34 result in higher p-values (less significance) for some of the higher thresholds. Further, WT3 is the other wet WT, which makes it a compelling covariate to select, because it develops a model with both precipitation scenarios experienced in NM, helping with interpretation. For these reasons, the PP model with Loc(WT4)+Scale(WT3) is selected for further investigation, though we acknowledge that there may not be a single "best" model, and another option could be to look at multiple models. Table 3 shows the parameter coefficients for the selected model: across all thresholds, the coefficient for the location parameter is positive and the coefficient for the scale parameter is negative. The shape parameter goes from positive to negative as the threshold increases, but all values are close to zero; further, the 95% confidence intervals for the shape parameter span across zero (not shown).

Next, the sensitivity of the selected PP model fit to the covariates is investigated. The frequency of exceedance, as calculated by the Poisson distribution, is most sensitive to the location parameter. Figure 8 shows how the frequency of exceedance varies across thresholds when the scale parameter (WT3) is held constant at its median value and the location covariate (WT4) is varied between the 5^{th} and 95^{th} percentile values. For the stationary fit with threshold = 6mm, the frequency of exceedance is about 4 days per season. However, given the positive coefficient on the location parameter (Table 3), it follows that when there are not very many WT4 days (e.g., 5^{th} percentile value), the frequency drops to about 2 days per season, versus when there are many WT4 days (e.g., 95^{th} percentile value), and it increases to 7 days.

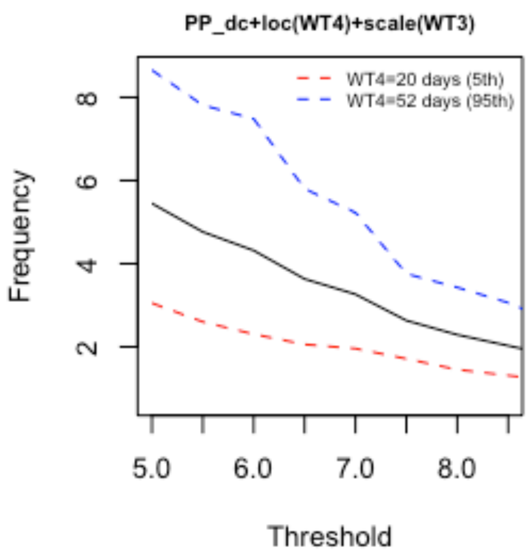

Figure 8. For the declustered Point Process (PP_dc) model with location (WT4) and scale (WT3), estimated frequency (days per monsoon season) of exceeding each threshold. Sensitivity is shown where location parameter varies to 95^{th} and 5^{th} percentile values, and scale stays at median value.

The conditional exceedance likelihood is sensitive to the scale parameter. Figure 9 shows the conditional exceedance likelihoods when the location covariate is held constant at the median and the sensitivity of the scale parameter using the 5^{th} and 95^{th} percentile values is examined. First, the conditional probability of exceeding 12 mm is checked: once 6mm is exceeded, there is an 18% chance of exceeding 12 mm in the stationary model. The conditional exceedance is influenced by the scale covariate, in this case WT3, which has a negative coefficient (Table 3). As such, when there are *fewer* WT3 days (e.g., 24 days), that chance *increases* to almost 25%, and similarly when there are *more* WT3 days (e.g., 49 days), it *decreases* to 9%. While this result may seem counterintuitive at first (i.e., fewer WT3 days leading to increased exceedance likelihood), WT3 has less intense precipitation than WT4; further, WT3 days and WT4 days are inversely correlated (r=-0.51, see Supplemental Figure 4.) If a more extreme value is analyzed, such as 25 mm (close to the Q100 of Figure 3), for 6mm, the stationary probability of exceedance is about 1%, and when WT3 is low (5^{th}), it is about 2% and when WT3 is high (95^{th}), it is an order of magnitude lower (0.2%). For the 6mm threshold, it is also possible to look at the return-level time series, which shows how the return levels vary over time (Supplemental Figure 5). Finally, it is important to look at the fit diagnostics, (Supplemental Figure 6 and 7), which indicate that the model is a reasonable fit.

Table 3. Estimated parameters for the PP model with location covariate of the sum of weather type 4 days over the season (WT4) and scale covariate of the sum of weather type 3 days over the season (WT3).

Threshold (mm)	Location (WT4)	Scale (WT3)	Shape
5	0.12	-0.073	0.041
5.5	0.12	-0.077	0.065
6	0.12	-0.071	0.103
6.5	0.11	-0.082	0.060
7	0.10	-0.062	0.134
7.5	0.10	-0.081	-0.013
8	0.11	-0.078	-0.019
8.5	0.10	-0.054	-0.001

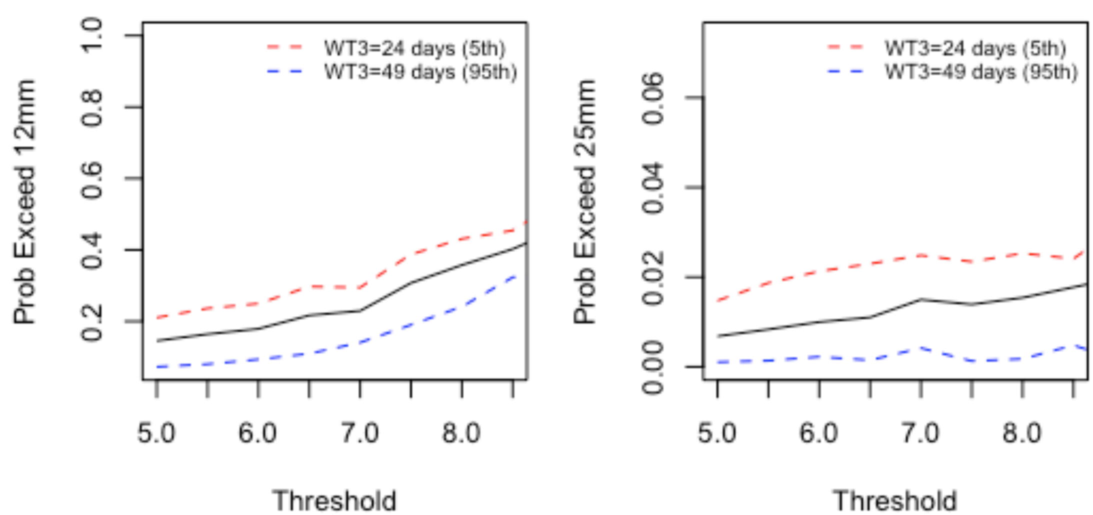

Figure 9. For the declustered Point Process (PP_dc) model with location (WT4) and scale (WT3), conditional probability of exceedance of 12 mm (left) and 25 mm (right); exceedance is conditional on the x-axis threshold being exceeded. Sensitivity is shown where scale parameter varies to 95^{th} and 5^{th} percentile values, and location stays at median value.

6. Downscaling with the PP Model for Water Management

In this study, the PP model is fitted to historical data, but it can also be used to downscale climate model projection data. To demonstrate this, the output from the Community Earth System Large Ensemble (CESM-LE; Kay et al. 2015) is utilized. The CESM-LE is a set of climate change projections, run from 1920 to 2100, and has 40 ensemble members that only differ slightly in their initial conditions to estimate climate internal variability. For each ensemble, the clustering algorithm (Prein 2019) is used to associate each day to one of the four WTs, but importantly, any trends in the three variables (PW, SLP, wind) are removed. Subsequently, only changes in the warm-season large-scale dynamics are considered and thermodynamic effects, such as the increase in PW, are eliminated. Therefore, this downscaling is likely conservative because thermodynamic effects can significantly increase precipitation rates (e.g., Kröner et al. 2017). The results for counting the number of WT3s and WT4s per monsoon season for each ensemble, and run through the final PP model with Loc(WT4)+ Scale(WT3) are shown in Figure 10. Selecting a threshold of 6mm, the frequency of exceedance exhibits an increasing trend after 2050, which is consistent with increasing frequency of WT4 patterns in the model. From this plot, it can also be seen that the model fitted historical frequencies are mostly within the inner quartile range (blue band). In terms of the conditional probability of exceeding 25mm, there is not much of a trend that can be seen in the CESM-LE, consistent with the fact that frequency of WT3 patterns stays relatively constant in the ensemble time series. Interestingly, the fitted model (red line) spans the inner quartile range (blue envelope) but also spans lower towards the minimum of the CESM-LE estimate, suggesting that the ensemble may be slightly overpredicting the likelihood of exceedance. The CESM-LE can help to provide context for historical as well as future extremes in this area, and provides a demonstration of its use as an extremes downscaling technique for water management.

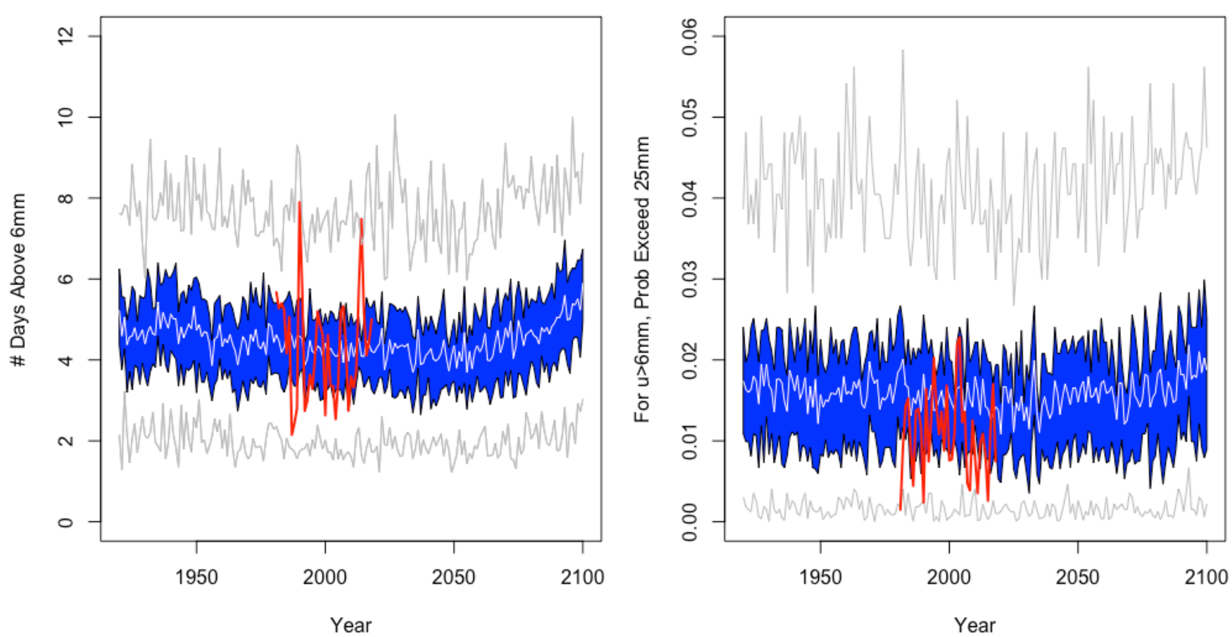

Figure 10. Using weather type data from the CESM-LE (Community Earth System Model Large Ensemble), the frequency of exceeding 6mm (left) and the conditional probability of exceeding 25mm if 6mm is exceeded. Grey lines

are ensemble min/max, blue envelop is 25th-75th percentile, white line is ensemble average, and red line is historical fitted.

7. Discussion and Conclusions

In this paper, a generalized workflow employing the PP modeling framework is developed. Of the extreme-value theory (EVT) tools, the non-stationary PP model is one of the more complex and has been used less extensively in water resources applications. This paper provides an end-to-end application of its development and demonstration. The workflow is demonstrated using precipitation extremes in a watershed in NM, where understanding the current risk profile and drivers of precipitation extremes is useful for understanding the opportunities and threats for water resource management and flood protection. The developed PP model is demonstrated for downscaling using a large ensemble climate projection dataset, which shows that the frequency of exceeding a high threshold increases after 2050, but the conditional likelihood of exceeding a very high threshold, such as the maximum observed, stays relatively constant. This result is consistent with other work that has found that trends are more detectible in frequency of extreme precipitation, rather than the magnitude (Pournasiri Poshtiri et al, 2018; Mallakpour & Villarini 2017). For water managers looking to exploit changes in precipitation for water supply, this behavior suggests that in a climatological sense across the watershed, there may be an increase in opportunities to harness more frequent extreme events. At the same time, this work suggests that managers may not need to plan for events larger than previously experienced. However, in this downscaling product, the WT information is employed to account for changes in large-scale dynamic drivers of extremes; increases in PW caused by warming (i.e., a thermodynamic driver) could lead to an increase in high-return period events.

Because the primary focus here was on the potential opportunities for water supply within the entire watershed attained from extreme values, spatial averaging of the gridded daily precipitation data is investigated. Perhaps the maximum over space is a better spatial summary to use when investigating the behavior of extreme values for flood risk, but for this study, it is sufficient. Gilleland et al. 2013a employ the Heffernan and Tawn (2004) model in order to account for spatial dependence across locations whereby the process-level dependence at each location is modeled using a spatial field energy. In their work, this energy was defined to be the upper quartile over space, but the spatial average could be used instead, and in that case, the extreme values are not lost because this variable is only used in capturing the spatial dependence structure.

The workflow could also be applied to data from a particular point (either gridded data or from an observational dataset), or in some cases applied to each grid point individually (e.g., Heaton et al. 2011), where a spatial model on the parameters of the GP and PP models was employed within a Bayesian hierarchical model (BHM), which accounts for some spatial dependence but not at the process level. In the field of spatial extremes, statistical tools have been brought to bear on the problem, including BHM (Cooley et al. 2007; Bracken et al. 2016), copulas, and max-stable random fields (see Davison et al. 2012 for a review); however, spatial extremes modeling is still an active area of research.

For the downscaling demonstration, here, a large ensemble climate projection is used, but note that this approach could be used on different projection datasets and/or prediction timescales. For instance, it could be applied with sub-seasonal to seasonal, annual, or decadal predictions as well; future work will be focusing on seasonal prediction. Specifically, the skill of the WT patterns could be assessed using existing seasonal forecast ensembles, such as the North American Multi-Model Ensemble (NMME). In the Rio Grande, as well as for other river basins in the Western U.S., warm-season precipitation and streamflow predictability has been elusive. This work on identifying large-scale monsoon circulation patterns and incorporating them into an extremes model to predict monsoon characteristics has shown promise in an area for which very little predictive information has been available in the past. Hence, the potential for the use of WTs to provide some robust seasonal predictability warrants further study, and is a critical step towards implementation. Reliable prediction of the characteristics of warm-season precipitation anomalies and extremes during a given year can help water managers make key operational and planning decisions.

Acknowledgements: This work was supported by the Bureau of Reclamation Science & Technology award No. 1782: “Detecting, Interpreting, and Modeling Hydrologic Extremes to Support Flexible Water Management and Planning.” This material is based upon work supported by the National Center for Atmospheric Research (NCAR), which is a major facility sponsored by the National Science Foundation (NSF) under Cooperative Agreement No. 1852977. Work for Eric Gilleland was funded by the NSF supported program at NCAR, the Regional Climate Uncertainty Program (RCUP).

References

Adams DK, Comrie AC (1997). The North American monsoon. Bulletin of the American Meteorological Society, 78(10): 2197-2213.

Bracken C, Rajagopalan B, Cheng L, Kleiber W, Gangopadhyay S (2016). Spatial Bayesian hierarchical modeling of precipitation extremes over a large domain. Water Resources Research, 52, 6643–6655. https://doi.org/10.1002/2016WR018768

Chavarria S, Gutzler DS (2017). Observed changes in climate and streamflow in the Upper Rio Grande Basin. Journal of the American Water Works Association, 54(3): 644-659.

Christensen JH, Krishna Kumar K, Aldrian E, An S-I, Cavalcanti IFA et al (2013). Climate phenomena and their relevance for future regional climate change. In: Stocker, TF, Qin D, Plattner G-K, Tignor M, Allen SK, Boschung J, Nauels A, Xia Y, Bex V, Midgley PM (eds.), Climate change 2013: the physical science basis. Contribution of working group I to the fifth assessment report of the intergovernmental panel on climate change. Cambridge University Press, Cambridge, United Kingdom and New York, NY, USA

Coles S (2001). An Introduction to Statistical Modeling of Extreme Values, Springer, London.

Collins M, Knutti R, Arblaster J, Dufresne J-L, Fichefet T et al (2013) Long-term climate change: projections, commitments. and irreversibility. In: Stocker TF, Qin D, Plattner G-K, Tignor M, Allen SK, Boschung J, Nauels A, Xia Y, Bex V, Midgley PM (eds), Climate Change 2013: The Physical Science Basis. Contribution of Working Group I to the Fifth Assessment Report of the Intergovernmental Panel on Climate Change. Cambridge University Press, Cambridge, United Kingdom and New York, NY, USA

Cooley D, Nychka D, Naveau P (2007). Bayesian spatial modeling of extreme precipitation return levels. Journal of the American Statistical Association, 102, 824–840.

Davison AC, Padoan SA, Ribatet M (2012). Statistical modeling of spatial extremes. Statistical Science, 27(2), 161–186.

Dee D, Uppalaa SM, Simmonsa AJ, Berrisforda P, Polia P, et al (2011). The ERA-Interim reanalysis: Configuration and performance of the data assimilation system. Quarterly Journal of the Royal Meteorological Society, 137 (656), 553–597.

Douglas MW, Maddox R, Howard K, Reyes S (1993). The Mexican monsoon. Journal of Climate, 6: 1665-1667.

Flato G, Marotzke J, Abiodun B, Braconnot P, Chou SC et al (2013). Evaluation of climate models. In: Stocker TF, Qin D, Plattner G-K, Tignor M, Allen SK, Boschung J, Nauels A, Xia Y, Bex V, Midgley PM (eds), Climate change 2013: the physical science basis. Contribution of working group I to the fifth assessment report of the Intergovernmental Panel on Climate Change. Cambridge University Press, Cambridge, United Kingdom and New York, NY, USA

Fowler H, Blenkinsop S, Tebaldi C (2007). Linking climate change modelling to impacts studies: recent advances in downscaling techniques for hydrological modelling. International Journal of Climatology, *27*, 1547–1578. https://doi.org/10.1002/joc

Gilleland E, Brown BG, Ammann CM (2013a). Spatial extreme value analysis to project extremes of large-scale indicators for severe weather. Environmentrics, DOI: 10.1002/env.2234

Gilleland E, Katz R (2016). extRemes 2.0: An Extreme Value Analysis Package in R. Journal of Statistical Software, 72(8), doi: 10.18637/jss.v072.i08.

Gilleland E, Ribatet M, Stephenson AG (2013b). A software review for extreme value analysis. Extremes, *16*, 103–119. https://doi.org/10.1007/s10687-012-0155-0

Gutmann E, Pruitt T, Clark M, Brekke L, Arnold J, Raff D, Rasmussen R (2014). An intercomparison of statistical downscaling methods used for water resource assessments in the United States. Water Resources Research, doi:10.1002/2014WR015559.

Gutzler DS (2013). Climate and drought in New Mexico. In: Water Policy in New Mexico [Brookshire, D.S., Gupta, H.V., and Matthews O.P. (eds.)]. RFF Press, New York, 72–86.

Heaton MJ, Katzfuss M, Ramachandar S,Pedings K, Gilleland E, Mannshardt-Shamseldin E, Smith RL (2011). Spatio-temporal models for large-scale indicators of extreme weather. Environmetrics, 22(3): 294–303.

Heffernan JE, Tawn, JA (2004). A conditional approach for multivariate extreme values (with discussion). Journal of the Royal Statistical Society: Series B (Statistical Methodology), **66**(3): 497– 546.

Katz RW, Parlange MB, Naveau P (2002). Statistics of extremes in hydrology. Advances in Water Resources, 25, 1287–1304.

Kay JE, Deser C, Phillips A, Mai A, Hannay C, Strand G, et al (2015). The Community Earth System Model (CESM) Large Ensemble Project: A Community Resource for Studying Climate Change in the Presence of Internal Climate Variability. Bull. Amer. Meteor. Soc. 96, 1333–1349. https://doi.org/10.1175/BAMS-D-13-00255.1

Kröner N, Kotlarski S, Fischer E, Lüthi D, Zubler E., Schär C (2017). Separating climate change signals into thermodynamic, lapse-rate and circulation effects: theory and application to the European summer climate. Climate Dynamics, 48(9-10), pp.3425-3440.

Kunkel KE, Andsager K, Easterling DDR. (1999). Long-term trends in extreme precipitation events over the conterminous United States and Canada. Journal of Climate, 12(1998): 2515–2527. https://doi.org/10.1175/1520-0442(1999)012<2515:LTTIEP>2.0.CO;2

Maraun D, Wetterhall F, Ireson AM, Chandler RE, Kendon EJ, Widmann M et al (2010). Precipitation downscaling under climate change: Recent developments to bridge the gap between dynamical models and the end user. *Reviews of Geophysics*, *48*(3), 1–34. https://doi.org/10.1029/2009RG000314

Mahoney K, Alexander M, Scott JD, Barsugli J (2013). High-resolution downscaled simulations of warm-season extreme precipitation events in the Colorado Front Range under past and future climates. Journal of Climate, DOI: http://dx.doi.org/10.1175/JCLI-D-12-00744.1

Mallakpour I, Villarini G (2017). Analysis of changes in the magnitude, frequency, and seasonality of heavy precipitation over the contiguous USA. Theoretical and Applied Climatology, 130(1–2), 345–363.

Pournasiri Poshtiri M, Towler E, Llewellyn D, Prein AF (2018). Extremes of opportunity: Examining recent trends in warm season extreme precipitation for New Mexico River Basins, 86th Western Snow Conference, Albuquerque, NM, https://westernsnowconference.org/files/PDFs/2018Poshtiri.pdf.

Powers JG, Klemp JB, Skamarock WC, Davis CA, Dudhia J, Gill DO, Coen JL, Gochis DJ, Ahmadov R, Peckham SE, Grell GA (2017). The weather research and forecasting model: Overview, system efforts, and future directions. Bulletin of the American Meteorological Society, 98(8), pp.1717-1737.

Prein AF, Holland GJ, Rasmussen RM, Done J, Ikeda K, Clark MP, Liu CH (2013). Importance of regional climate model grid spacing for the simulation of heavy precipitation in the Colorado headwaters. J Clim, 26(13), 4848-4857.

Prein AF (2019). The changing character of the North American Monsoon and its impacts on New Mexico's precipitation. Journal of Climate, submitted.

Prein AF, Bukovsky MS, Mearns LO, Bruyère C, Done JM (2019). Simulating North American weather types with regional climate models. Frontiers in Environmental Science, 7, p.36.

Prein AF, Holland GJ, Rasmussen RM, Clark MP, Tye MR (2016). Running dry: The US Southwest's drift into a drier climate state. Geophysical Research Letters, 43(3), pp.1272-1279.

R Core Team (2019). R: A language and environment for statistical computing. R Foundation for Statistical Computing, Vienna, Austria, https://www.R-project.org/.

Reiss RD, Thomas M (2007). Statistical Analysis of Extreme Values: With Applications to Insurance, Finance, Hydrology and other Fields. 3rd edition. Birkhauser.

Seneviratne SI, Nicholls N, Easterling D, Goodess CM, Kanae S et al (2012). Changes in climate extremes and their impacts on the natural physical environment. In: Managing the Risks of Extreme Events and Disasters to Advance Climate Change Adaptation [Field CB, Barros V, Stocker TF, Qin D, Dokken DJ, Ebi KL, Mastrandrea MD, Mach KJ, Plattner G-K, Allen SK, Tignor M, Midgley PM (eds.)]. A Special Report of Working Groups I and II of the Intergovernmental Panel on Climate Change (IPCC). Cambridge University Press, Cambridge, UK, and New York, NY, USA, pp. 109-230.

Skamarock WC, Klemp JB, Dudhia J, Gill DO, Barker DM, Wang W, Powers JG (2005). A description of the advanced research WRF version 2 (No. NCAR/TN-468+ STR). National Center for Atmospheric Research Boulder Co Mesoscale and Microscale Meteorology Div.

Soden BJ, Held IM (2006). An assessment of climate feedbacks in coupled ocean–atmosphere models. Journal of Climate, 19(14), pp. 3354-3360.

Towler E, Llewellyn D, Barrett L, Young R (2019). Extremes of Opportunity? A generalized approach to identify intersections between changing hydrology and water management. Proceedings of the Federal Interagency Sedimentation and Hydrologic Modeling Conference (SEDHYD) Conference, Reno, NV. Available at: https://www.sedhyd.org/2019/openconf/modules/request.php?module=oc_program&action=view.php&id=160&file=1/160.pdf

Vigaud, N., Robertson, A.W., Tippett, M.K. and Acharya, N., 2017. Subseasonal predictability of boreal summer monsoon rainfall from ensemble forecasts. Frontiers in Environmental Science, 5, p.67.

Villarini G (2016). On the seasonality of flooding across the continental United States. Advances in Water Resources, 87: 80–91. http://doi.org/10.1016/j.advwatres.2015.11.009

Wilby RL, Charles SP, Zorita E, Timbal B, Whetton P, Mearns LO (2004) Guidelines for use of climate scenarios developed from statistical downscaling methods, technical report, Intergovt. Panel on Climate Change, Geneva, Switzerland

Supplemental Figures

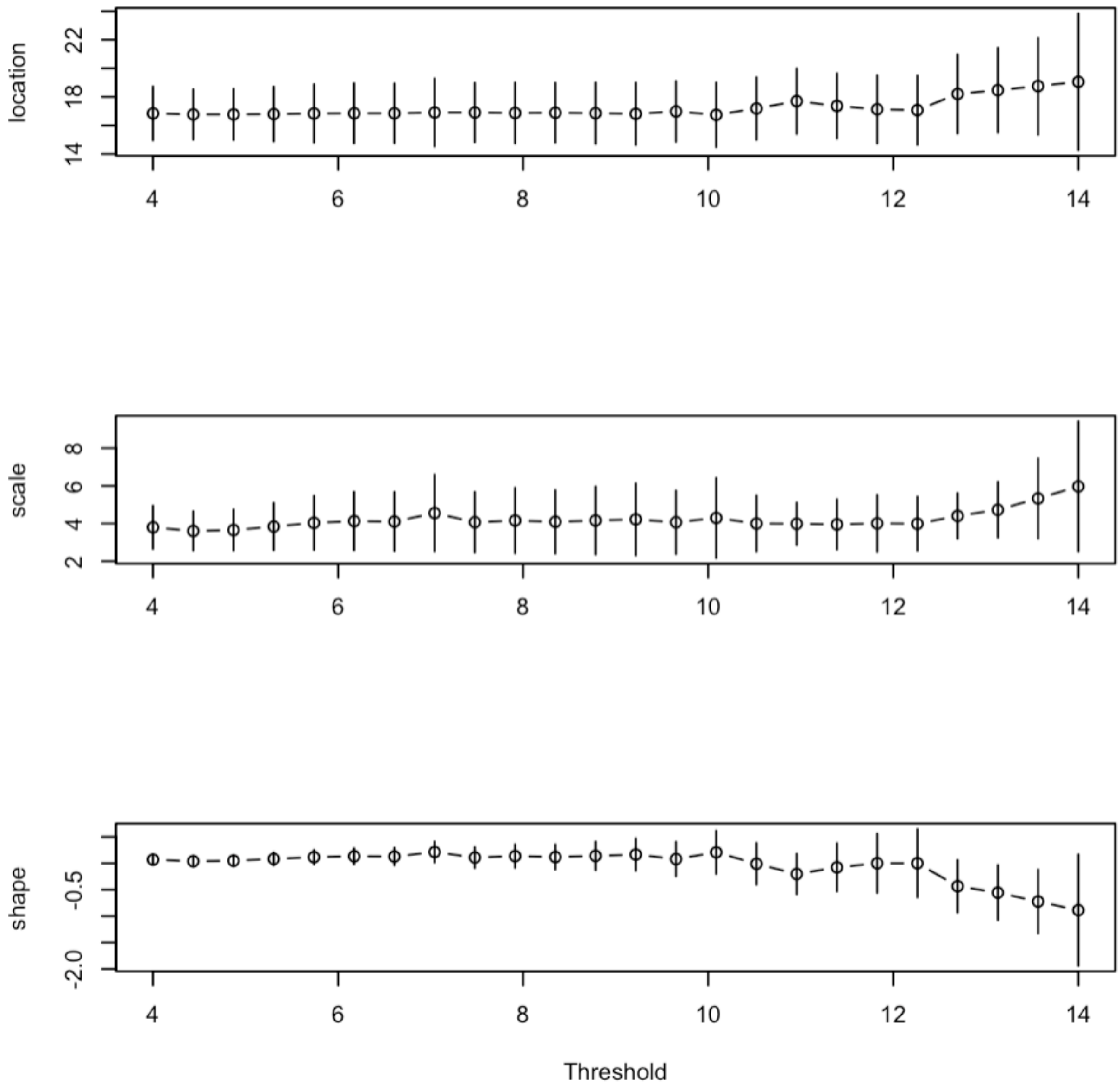

Supplemental Figure 1. For Point Process (PP) model fit, parameter estimates for location, scale, and shape over a range of thresholds.

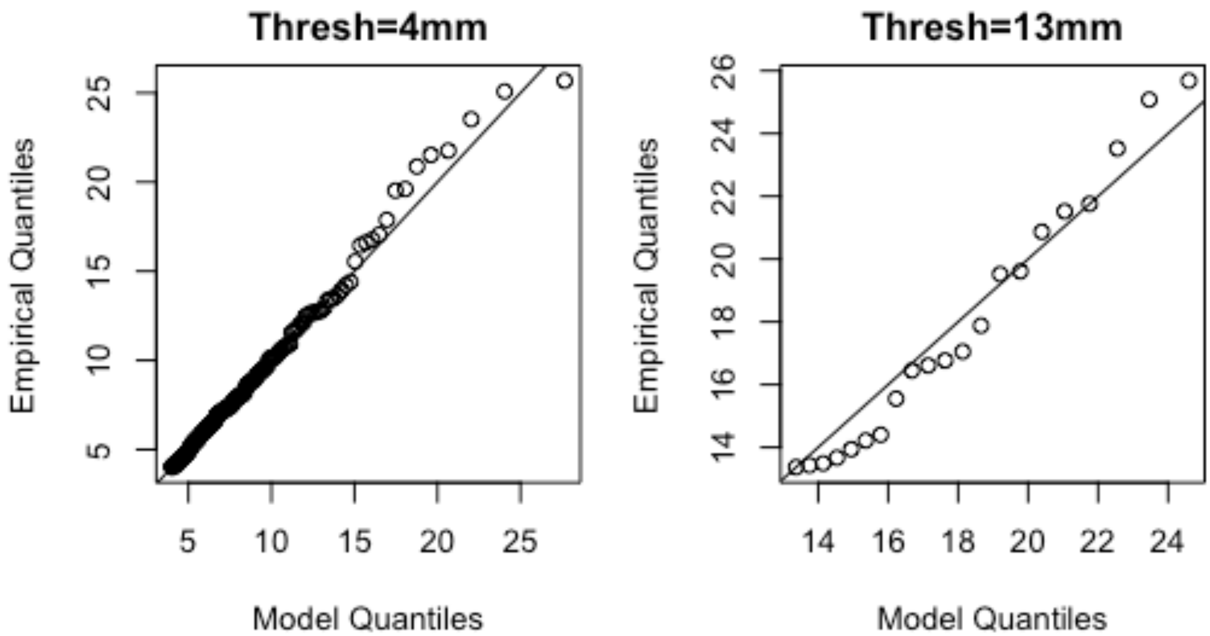

Supplemental Figure 2. Quantile-quantile (QQ) plot of the data quantiles against the fitted model quantiles for 4mm (left) and 13 mm (right).

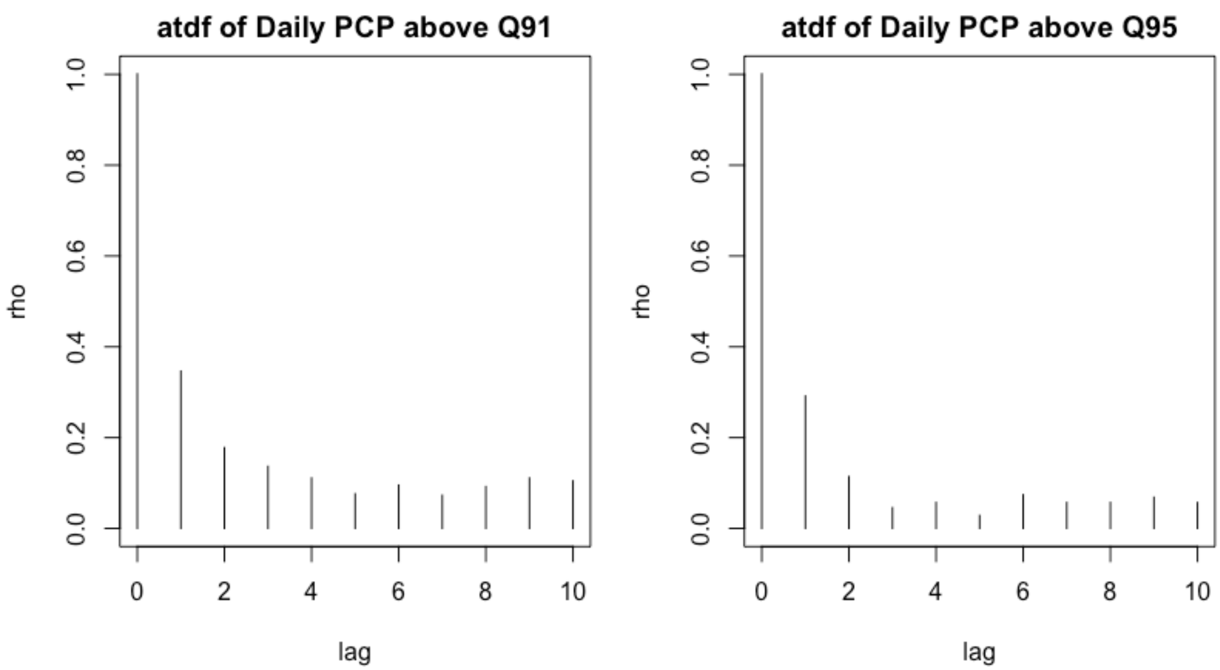

Supplemental Figure 3. Auto-tail dependence function (atdf) of different thresholds (Q91=5mm and Q95=7mm) showing the dependence in the precipitation extremes.

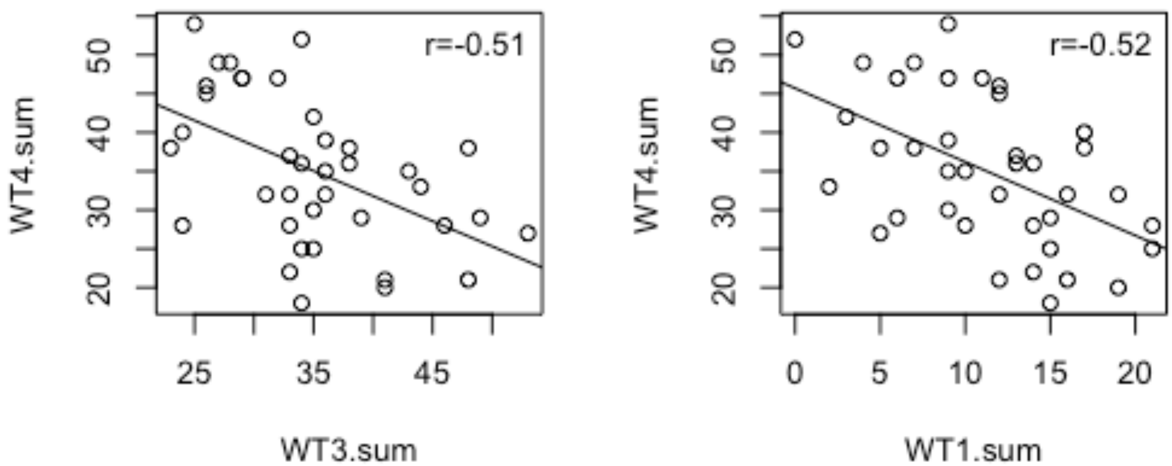

Supplemental Figure 4. Relationship between sum of weather type 3 days (WT3.sum) and weather type 4 days (WT4.sum) (left), and weather type 1 days (WT1.sum) and WT4.sum; r is linear correlation coefficient.

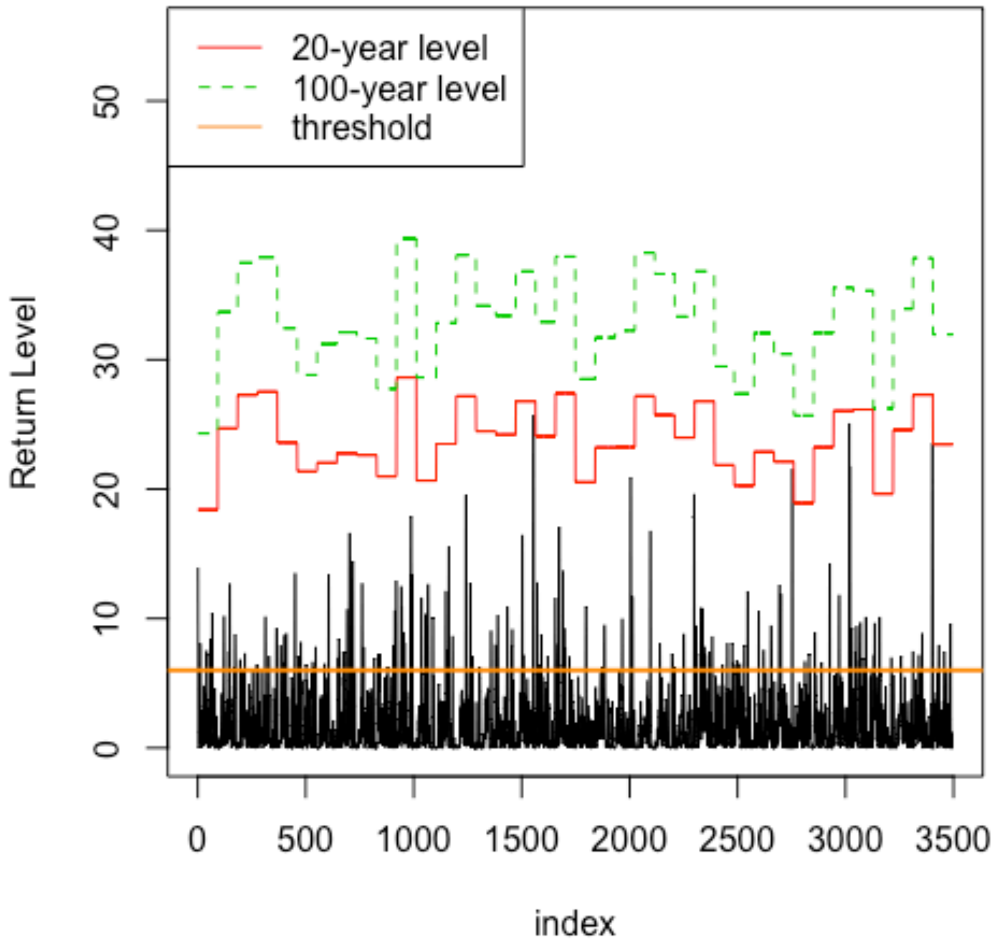

Supplemental Figure 5. Return level time series for final model with WT4 in location and WT3 in scale for threshold = 6mm.

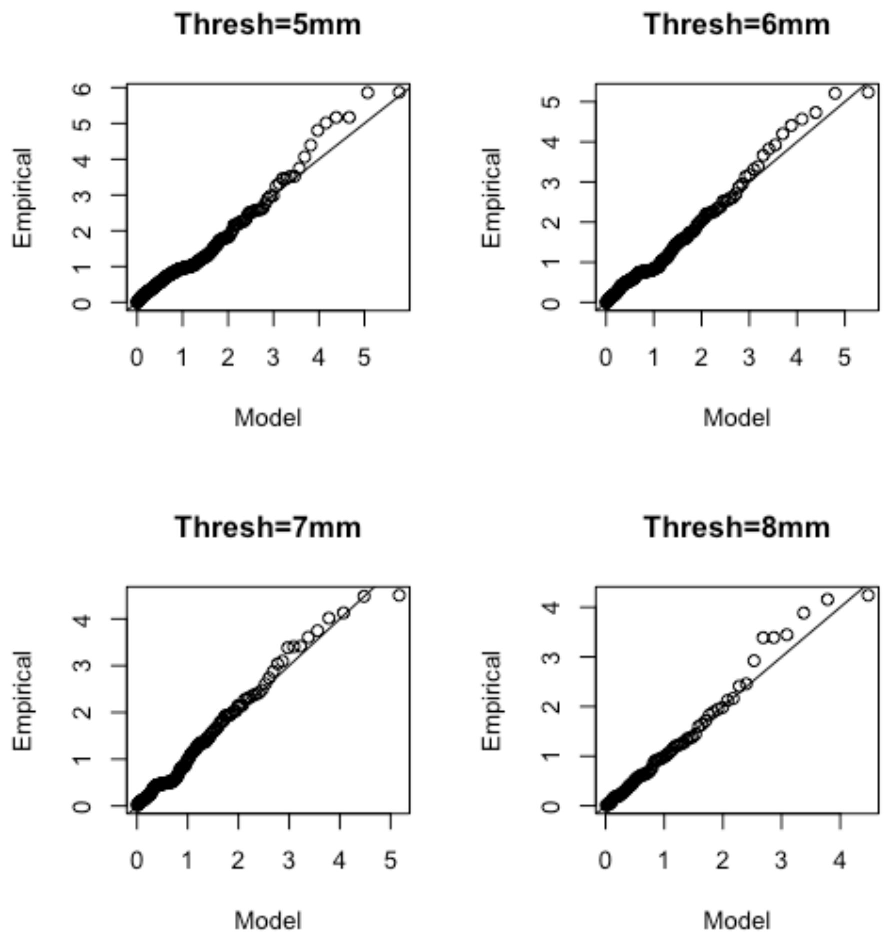

Supplemental Figure 6. Quantile-quantile (QQ) plot of the data quantiles against the fitted model quantiles.

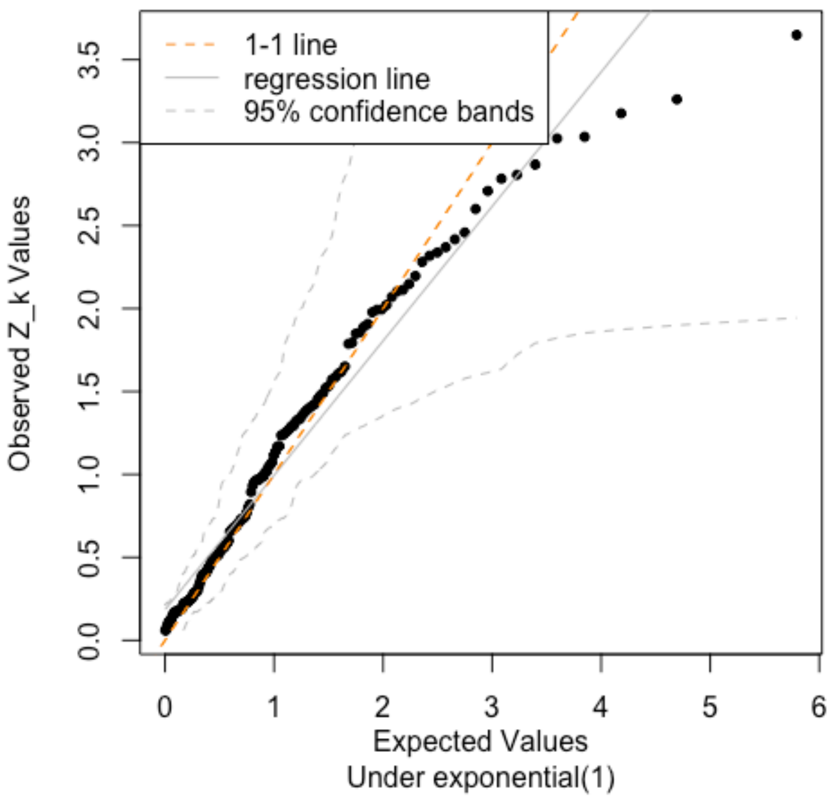

Supplemental Figure 7. Zplot for threshold = 6mm; this is a diagnostic for the PP model based on Smith and Shively (1995); Smith, R. L. and Shively, T. S. (1995). A point process approach to modeling trends in tropospheric ozone. *Atmospheric Environment*, **29**, 3489–3499.

Supplemental Tables

Supplemental Table 1. Comparing the raw to declustered daily data in terms of extremal index, Akaike Information Criterion (AIC) values from the stationary Point Process fit, and percent of data points retained after declustering.

	Extremal Index		AIC		Data Retained (%)	
Threshold	Raw	Declustered	Raw	Declustered	Raw	Declustered
5	0.694	1	674	667	318 (9.1%)	207 (5.9%)
5.5	0.686	1	643	631	282 (8.1%)	181 (5.2%)
6	0.755	1	623	597	241 (6.9%)	164 (4.7%)
6.5	0.789	1	606	561	198 (5.7%)	138 (4.0%)
7	0.808	1	565	522	175 (5.0%)	124 (3.6%)
7.5	0.738	1	538	484	137 (3.9%)	100 (2.9%)
8	0.808	1	500	449	115 (3.3%)	87 (2.5%)
8.5	0.787	1	463	416	103 (3.0%)	77 (2.2%)
9	0.756	0.97	425	383	85 (2.4%)	67 (1.9%)
9.5	0.815	1	388	351	72 (2.1%)	58 (1.7%)
10	0.855	1	358	327	64 (1.8%)	53 (1.5%)
10.5	0.811	0.93	318	294	50 (1.4%)	44 (1.3%)
11	0.851	0.97	284	262	41 (1.2%)	36 (1.0%)
11.5	0.873	0.97	273	254	40 (1.1%)	36 (1.0%)
12	1	1	246	231	34 (1.0%)	31 (0.9%)

Supplemental Table 2. Akaike Information Criterion (AIC) values for all model combinations considered in Step 5.5. of manuscript; red indicates lowest AIC value by threshold.

Model		Threshold							
Location	Scale	5	5.5	6	6.5	7	7.5	8	8.5
-	-	667	631	597	561	522	484	449	416
PW_avg	-	657	620	583	552	515	482	447	416
PW_avg	WT1	651	615	582	554	517	484	449	417
PW_avg	WT3	653	616	582	551	516	482	448	417
PW_avg	WT34	650	614	581	552	516	483	448	417
WT1	-	652	617	586	556	519	484	448	416
WT1	WT1	651	616	585	556	521	486	450	418
WT1	WT3	651	617	587	556	521	484	450	418
WT1	WT34	649	614	583	553	519	485	449	418
WT2	-	664	628	594	559	521	485	450	418
WT2	WT1	650	614	583	555	520	485	450	418
WT2	WT3	661	626	595	559	523	486	451	420
WT2	WT34	649	614	583	553	519	485	450	418
WT34	-	653	618	586	554	518	484	449	417
WT34	WT1	650	615	584	555	520	485	450	418
WT34	WT3	653	618	587	555	520	485	450	419
WT34	WT34	650	615	583	553	519	485	450	418
WT4	-	664	628	592	558	519	484	447	414
WT4	WT1	651	616	585	556	519	485	449	416
WT4	WT3	648	613	582	550	517	481	446	415
WT4	WT34	650	615	583	553	518	485	448	416

Supplemental Table 3. p-values from likelihood ratio test for PP models for different combinations of location and scale. Red indicates p-value <=0.05.

Threshold (mm)	PP_dc+Loc(WT1)				PP_dc+Loc(WT34)				PP_dc+Loc(WT2)			
	-	+sca(WT3)	+sca(WT1)	+sca(WT34)	-	+sca(WT3)	+sca(WT1)	+sca(WT34)	-	+sca(WT3)	+sca(WT1)	+sca(WT34)
5	0	0.06	0.09	0.03	0	0.11	0.02	0.02	0.03	0.03	0	0
5.5	0	0.1	0.07	0.02	0	0.18	0.03	0.03	0.03	0.05	0	0
6	0	0.38	0.09	0.02	0	0.59	0.06	0.03	0.03	0.32	0	0
6.5	0.01	0.16	0.27	0.04	0	0.29	0.22	0.07	0.07	0.16	0.01	0
7	0.03	0.66	0.6	0.15	0.02	0.92	0.43	0.23	0.14	0.78	0.05	0.03
7.5	0.13	0.26	0.75	0.4	0.14	0.34	0.5	0.41	0.41	0.24	0.18	0.15
8	0.11	0.47	0.58	0.37	0.15	0.6	0.35	0.32	0.48	0.41	0.12	0.12
8.5	0.17	0.88	0.62	0.58	0.27	0.96	0.36	0.47	0.67	0.72	0.17	0.22

Appendix D – Component 4 Paper

Extremes of Opportunity? A generalized approach to identify intersections between changing hydrology and water management.

Erin Towler[1], Dagmar Llewellyn[2], Lucas Barrett[2], Rick Young[2]

[1] National Center for Atmospheric Research (NCAR), Boulder, CO

[2] Bureau of Reclamation, Albuquerque, NM

Paper published in the Proceedings of the Federal Interagency Sedimentation and Hydrologic Modeling Conference (SEDHYD) 2019

Abstract

For water managers, changing hydrology can underscore existing vulnerabilities as well as offer new opportunities. The purpose of this paper is to put forth a generalized approach to identify potential intersections between changing hydrology and water management. The generalized approach includes 4 steps: (i) Articulate management vulnerabilities and opportunities, (ii) Quantify current water contributions from sources that may provide the hydrologic opportunity, (iii) Identify key climatic and atmospheric drivers of the hydrologic opportunity, and (iv) Explore the opportunity-management nexus. The framework is demonstrated using a case study example of the Middle Rio Grande Basin of New Mexico and its downstream delivery point, Elephant Butte Reservoir. In Step 1, we articulate how New Mexico's water supplies are vulnerable to decreasing snowpack, but also that the summer monsoon season could offer a potential, currently under-developed, water supply opportunity. In Step 2 we examine historical Elephant Butte Reservoir inflows and find that although monsoon season volumes vary from year-to-year, they are an important contribution to annual water supply. Further, we find that the upper percentile inflows contribute a disproportionately larger fraction of the monsoon volume relative to their frequency of occurrence. Step 3 examines possible climate and atmospheric drivers for different characteristics of monsoon season interannual variability, finding that most monsoon inflow characteristics show a strong association with average precipitation over the contributing watershed and atmospheric precipitable water. In Step 4 we suggest how this information could be integrated into existing planning and operations for the Rio Grande Basin.

1. Introduction

In many river basins in the Western United States, snowmelt provides the primary contribution to water supply (Serreze 1999); hence, most reservoirs are designed to capture snowmelt runoff. However, increasing temperatures (Hayhoe et al. 2018) and decreasing snowpack (Mote et al. 2005, 2018) have already been observed across the Western United States (US), and general circulation models predict that these trends will continue into the future (Collins et al., 2013).

Taken together, these changes suggest increasing threats to water storage and availability in these reservoirs (Barnett et al. 2005). It is generally thought that increasing greenhouse gases will lead to an intensification of the hydrologic cycle, with an increase in heavy precipitation, potentially increasing local runoff (Seneviratne et al. 2012). In addition to posing flooding threats, these potentially increasing extreme precipitation events present opportunities to mitigate the impacts of decreasing snowmelt runoff volumes on water supply. However, the relevance of changing hydrology, including extremes, will depend on the particular water management context. As such, the purpose of this paper is to put forth a generalized approach to identify potential intersections between changing hydrology and water management.

The generalized approach includes 4 steps: (i) Articulate management vulnerabilities and opportunities, (ii) Quantify current water contributions from sources that may provide hydrologic opportunities, (iii) Identify key climatic and atmospheric drivers of the hydrologic opportunity, and (iv) Explore the opportunity-management nexus. In this paper, we first present the generalized framework (Section 2), which is demonstrated using a case study example of a reservoir in the Rio Grande Basin, New Mexico. This is followed by discussion and conclusions (Section 3).

2. Framework to Identify Intersections

2.1 Step 1. Articulate management vulnerabilities and opportunities

The relevance of changing hydrology is dependent on the particular water management context. Articulating local management vulnerabilities and potential opportunities is a critical first step towards adaptation planning. In this step, we provide background information on climate and water resources for New Mexico basins that include projects managed by the US Bureau of Reclamation.

2.1.1. Background: Similar to many water systems in the Western US, one key vulnerability for New Mexico is decreasing snowpack. Snowpack provides the main water source for most of the New Mexico river basins that begin in Colorado, (including the Rio Grande, San Juan, and Chama Rivers) and northern New Mexico (such as the Pecos River) (Gutzler 2013). As such, most of the reservoirs in these river systems are designed to capture snowmelt runoff, with storage located in the headwaters of the basins where temperatures and evaporation rates are lower (Gutzler 2013). Recent work by Chavarria and Gutzler (2018) has shown decreasing snowpack and increasing temperatures in the upper Rio Grande, resulting in slight decreases in snowmelt runoff. Further, they found that small precipitation increases have offset the impact of decreasing snowpack (Chavarria and Gutzler 2018). However, there is growing evidence that runoff efficiencies in the basin are becoming more sensitive to temperature (Lehner et al. 2017).

Rivers that originate further south in the state get a smaller proportion of their flow from snowpack, and warm season precipitation increases in importance. Warm-season precipitation has historically provided a secondary water source in the Western US (Serreze et al., 1999). If the total volume of this secondary supply were to increase in response to increasing ocean and air temperatures, warm-season precipitation could provide a potential water-supply opportunity for

New Mexico, which might make up, at least in part, for decreasing supplies from snowmelt runoff. In summer, the central and southern parts of the state are influenced by the North American Monsoon (Gutzler 2013; Adams and Comrie 1997), which result in significant contributions to annual precipitation (Douglas et al. 1993). Tropical cyclones also contribute during this time, though much less (<10%) during the main monsoon period (June 15-Sept 30), and more (up to 80%) in the relatively dry month of October (Wood and Ritchie 2013). For New Mexico, most extreme precipitation occurs in summer, followed by fall (Kunkel et al. 1999), and most flooding has been observed in summer (Villarini, 2016). Pournasiri Poshtiri et al (2018) examined recent trends in warm season precipitation characteristics, including extremes, and found that negative trends dominate warm season, June, and August, while positive trends dominate July and for some September precipitation characteristics. However, the majority of locations in New Mexico do not exhibit significant trends. The increasing trends for the July indicators show the most potential for water supply, with the location of these significantly positive trends mainly concentrated in the southeastern and eastern part of New Mexico. They also found that trends are more detectable in the frequency of extreme precipitation rather than the magnitude, similar to the findings of Mallakpour & Villarini (2017). As such, for times and locations showing increasing trends, their results suggest that water managers looking to exploit changes in precipitation might not need to plan for larger events, but rather for more frequent events.

The coarse resolution of general circulation models, which are typically used as a basis for projections of future climate and hydrology, limit the ability of these models to resolve monsoonal patterns. Therefore, there is currently low confidence in our ability to project changes in monsoonal patterns as the climate warms (Seneviratene et al. 2012). For parts of the US Southwest, projections for winter and spring seasons at the end of the century (2070-2099) show decreasing precipitation, though changes for this region in all seasons are small and relatively insignificant (Hayhoe et al. 2018). However, some past research (e.g., Asmerom et al., 2013) has suggested a correlation between ocean temperature and monsoon intensity. Seneviratne et al. (2012) recommend that any examination of monsoonal changes should consider large-scale circulation and dynamics, rather than solely examining precipitation. Examining current and future weather patterns, Prein 2018 finds a robust signal for an increase in the frequency of monsoonal circulations in New Mexico, particularly monsoonal patterns that contribute to the majority of monsoon season precipitation, as well as heavy precipitation events.

If Prein's conclusions are correct, there may be opportunities to exploit changes in warm season precipitation for water management (Gutzler, 2013, Llewellyn & Vaddey, 2013), warranting further investigation.

2.2. Step 2. Quantify current water contributions from sources that may provide hydrologic opportunities.

Quantifying the current contribution of water sources that might provide future water supply opportunities provides a critical baseline to which future climate or infrastructure scenarios can be compared. As articulated in Step 1, given decreasing snowpack, a potential opportunity for

New Mexico could be moisture from the monsoon season. In this section we provide an example of quantifying current monsoon season contributions to annual water supply.

As a case study, we examine the Middle Rio Grande Basin of New Mexico and its downstream delivery point, Elephant Butte Reservoir, located in the south-central New Mexico (see Figure 1). This reservoir provides significant water storage (up to approximately 2 million acre feet) for both snowmelt runoff and summer precipitation events. The analyses in Step 2 rely on the following dataset and definitions:

- Elephant Butte Reservoir inflows: Data are available from 2000-2017, and are calculated as the sum of the Rio Grande Low Flow Conveyance Channel at San Marcial and the Rio Grande Floodway at San Marcial (URGWOM Technical Team, 2005).
    - Monsoon season volume: We define the monsoon season volume as the sum of Elephant Butte Reservoir inflows from July 1 through September 30 (Jul-Sep). Initial analyses also included June 15-June 30, a time period that is often considered to be part of the monsoon season, but here it was found that that these inflows were still influenced by snowmelt.
    - Annual volume: We define the annual volume to be the sum of Elephant Butte Reservoir inflows during the calendar year (Jan-Dec).
    - Percentile-based indices: The definition of an extreme inflow at a particular location is site-specific; hence, percentile-based indices can be calculated from the historical Elephant Butte Reservoir inflows. We examine several percentiles: P99 is the 99th percentile flow, i.e., the value at which only 1% of daily inflows are higher. Similarly, we examine P95 (the 95th percentile, where only 5% of the daily inflows are higher), P90 (the 90th percentile), P75 (the 75th percentile), and P50 (the 50th percentile, or median daily flow).

In this step, we look at the interannual variability of monsoon season volumes and their contribution to annual inflows to Elephant Butte Reservoir (2.2.1), as well as the relationship between monsoon season volumes and upper percentile thresholds/extremes (2.2.2) and frequency and magnitude characteristics (2.2.3).

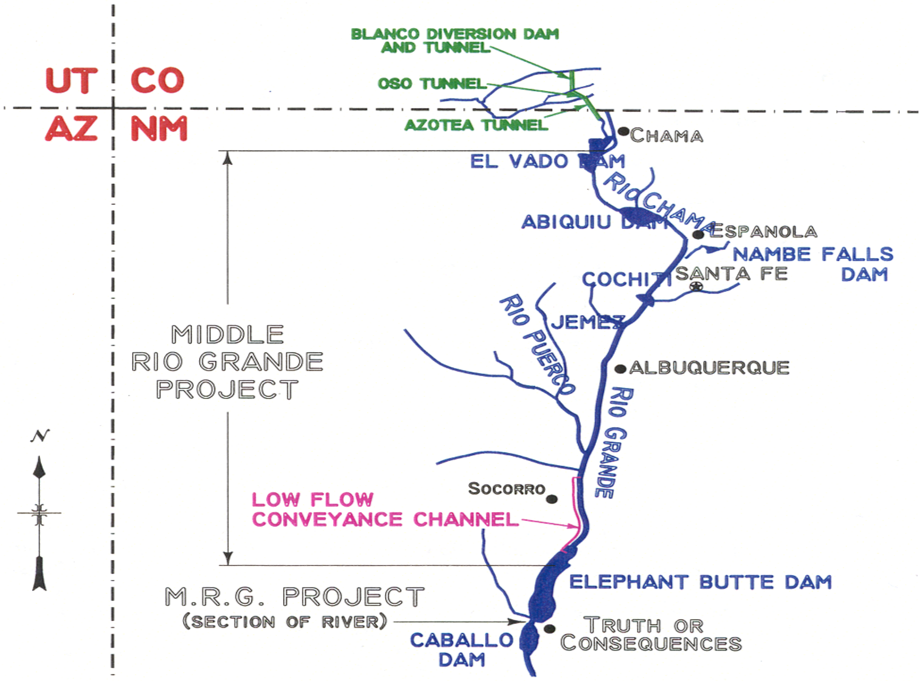

Figure 1. Map of Middle Rio Grande Basin of New Mexico and its downstream delivery point, Elephant Butte Reservoir, New Mexico.

2.2.1. Monsoon season volumes vary from year-to-year, but they are an important contribution to annual water supply: The interannual variability of Elephant Butte Reservoir inflows and storage volumes play a role in the operations and management decisions in the basin. Figure 2a (left) shows the annual monsoon season volumes for the 2000-to-2017 period analyzed; the average volume is about 68,383 acre-feet (af), the minimum was 16,432 af in 2003 and the maximum was 254,214 af in 2006. It is also useful to look at the contribution of the monsoon volume to annual volume, as in some years, even relatively low volumes may provide critical contributions. Figure 2b (right) shows that on average, monsoon volumes provide 14.4% of the annual supply, with a minimum of 4.00% in 2017 and a maximum of 43.6% in 2006. There is no statistically significant trend to the contribution, though it is hard to tell with the short sample size (18 years).

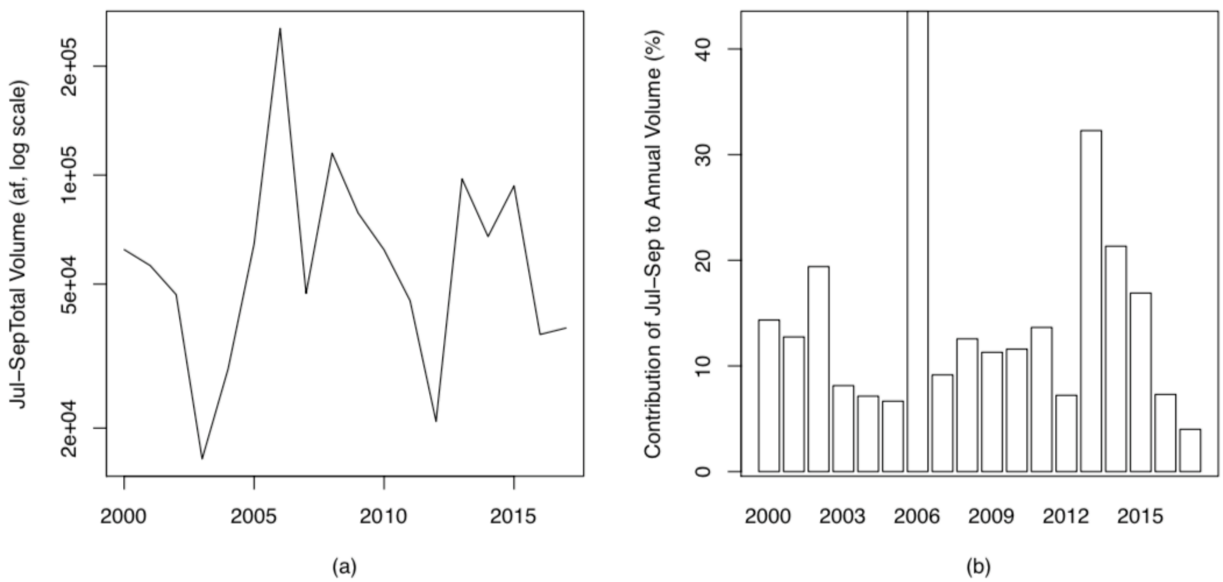

Figure 2. Monsoon (Jul-Sep) total volume in Elephant Butte Reservoir (a) and proportion of annual volume (Jan-Dec) coming from that year's monsoon (Jul-Sep) volume (b).

2.2.2. Inflows from upper percentiles contribute a disproportionately higher proportion of the monsoon volume relative to their occurrence: The percentile indices for the Elephant Butte daily inflows from the monsoon season (i.e., n = 1656 daily inflows) can be seen from the flow duration curve (Figure 3). Figure 3 shows that the upper half of daily inflows span an order of magnitude in volume: the 50th percentile (P50) is 452 acre feet and the 99th percentile (P99) is 5660 acre feet. The maximum daily flow in the analyzed period of record is 11,910 acre feet (in 2006; not shown in Figure 3). We also see that the 75th percentile (P75) for the inflows marks an inflection point: here, the absolute value of the slope starts to increase towards the higher percentiles (moving to the left in Figure 3), indicating a rapid shift towards higher daily inflows. Using these percentiles, we can look at the contribution of daily inflows above each percentile in each monsoon season (Figure 4). In Figure 4, the boxplots are comprised of the annual contributions from each percentile, hence the sample size, N, number of years, decreases; this is as expected, since the exceedance of the higher percentile indices does not occur in every year. As indicated by the median (horizontal line in box plots), the summed volumes from daily flows from the upper half of the distribution (>P50) contribute to 78% of the monsoon reservoir volume. Summed volumes from the top quarter (>P75) of daily inflows contributed 47% of monsoon reservoir volumes; top decile (>P90) of daily inflows contributed 28% of monsoon reservoir volumes. However, there is quite a bit of variability in the contribution from year-to-year for these percentiles (P50-P90). As we move into the higher, more extreme quantiles, these also play a role, but in fewer years. i.e., daily inflows above P99 are contributing disproportionately given their low occurrence, but only in the two years that they occur: this 1% occurrence accounts for 41% in 2006 and 23% in 2013 (resulting in a 32% median). The previously mentioned maximum daily inflow on record (e.g., 11,910 af), which occurred in August of 2006, contributed 5% of that year's monsoon reservoir volume.

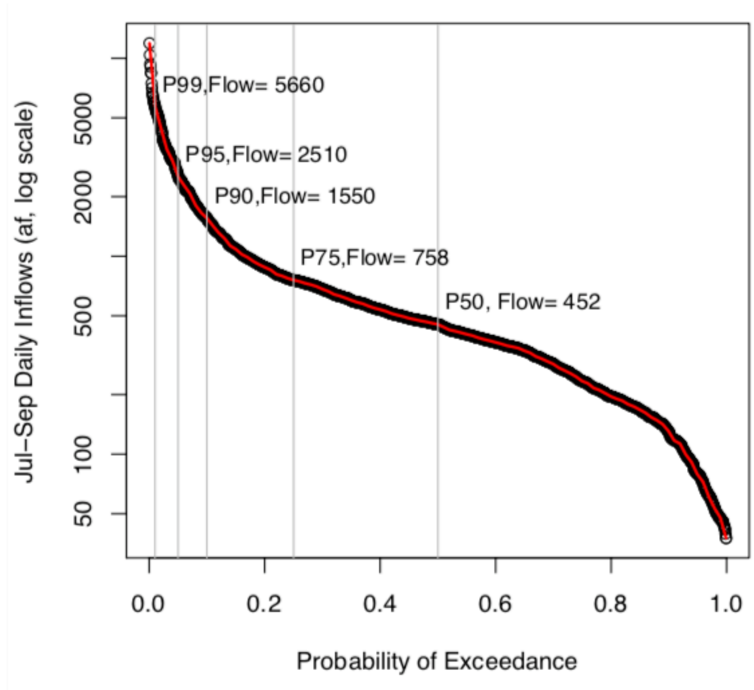

Figure 3. Flow duration curve of monsoon (Jul-Sep) daily inflows in acre feet (af; n=1656 days), with daily values of select percentile-based flow indices (P50, P75, P90, P95, P99), and smoothed spline (red line).

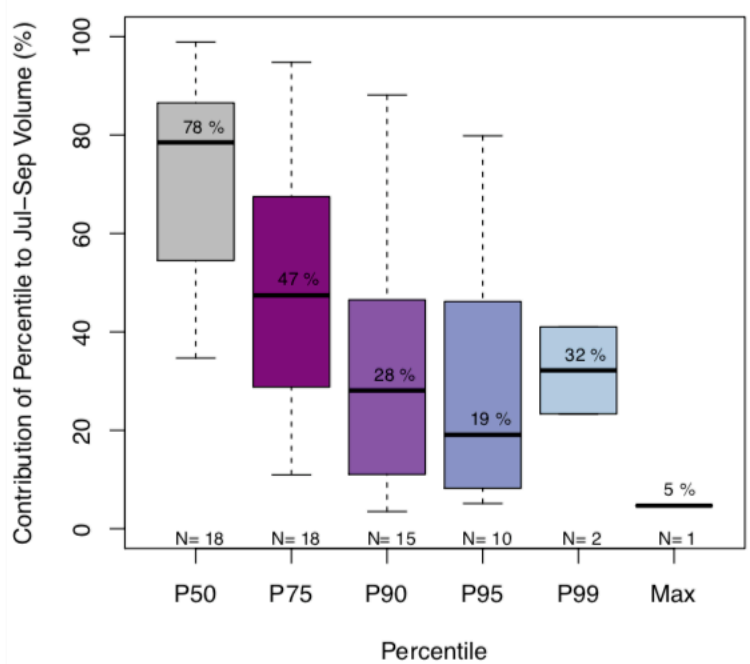

Figure 4. Proportion of monsoon (Jul-Sep) volume coming from daily inflows above each percentile-based flow index; P50 is the 50th percentile, P75th is the 75h percentile, and so on; Max is the maximum daily inflow. N is the number of years from which the daily inflows above the percentiles were observed.

2.2.3. Frequency and magnitude inflow characteristics partially explain interannual monsoon variability: We can also examine how well other inflow characteristics based on the percentile-based indices explain the interannual variability of monsoon reservoir volumes. Here we look at two characteristics: first, the frequency, or the number of days that the daily inflows were above the percentiles during the monsoon season. Figure 5 shows how the number of days above P50, P75, P90, and P95 relates to that year's monsoon reservoir volume. As we would expect, as the number of exceeding days increases, so does the total monsoon inflow volume. We see strong linear correlations, as measured by Pearson's r values, and find that the number of days above P75 has a stronger correlation (r=0.85) than P50 (r=0.62), showing the importance of the count of days in the upper quarter of the inflow distribution to total monsoon season volume. The number of days above P90 and P95 also have high correlations (r = .97 and .96, respectively), but here the linear correlations don't tell the whole story: the scatterplots reveal that there are several years with zero days above these thresholds. This relates to our previous point that these flows can be pivotal, but only in years in which they occur. The second characteristic that we examine is the annual magnitude, i.e., the value of the percentile index calculated annually for each monsoon season. For clarity, these are labeled $P50_{annual}$., $P75_{annual}$, and so on, indicating that these magnitudes are calculated from a flow duration curve like Figure 3, but for each year's monsoon season. The scatterplot in Figure 6 shows the association between the annual percentiles and that year's monsoon reservoir volume. These all exhibit very high linear correlations (r=0.95 to 0.98), indicating that these annual percentiles do a good job at explaining the interannual monsoon variability.

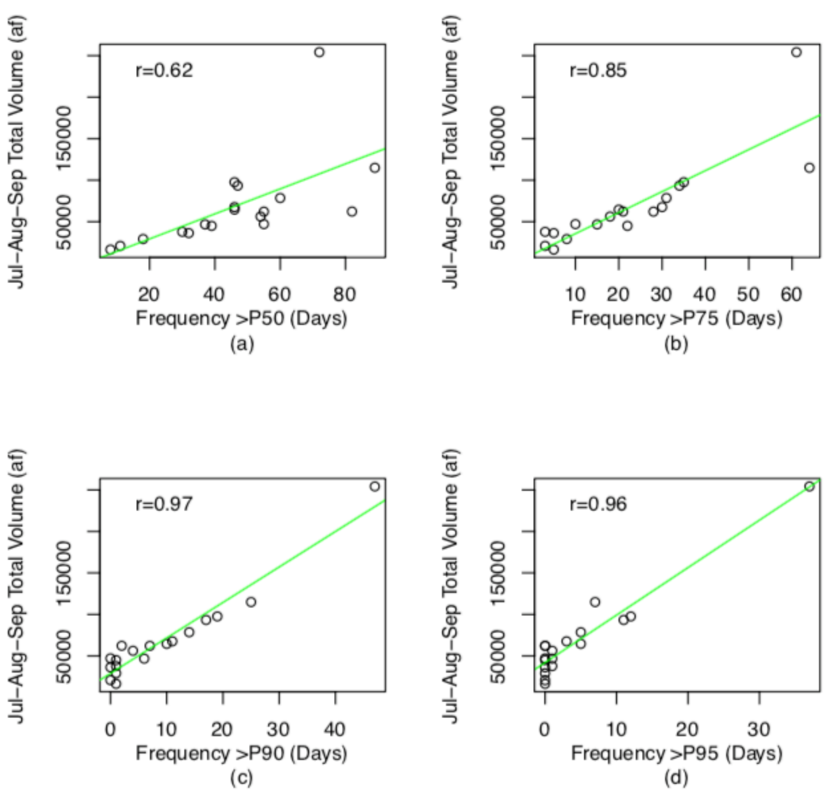

Figure 5. Frequency of days with inflows above select percentile-based indices versus monsoon (Jul-Sep) volumes in acre-feet (af); r is Pearson's linear correlation.

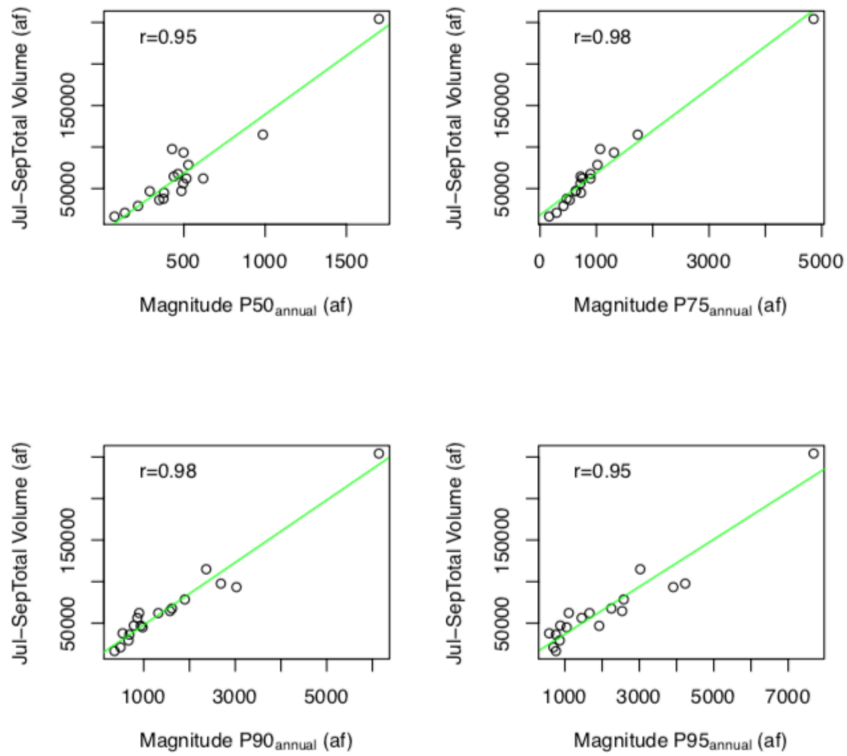

Figure 6. Inflow magnitudes of annual percentile-based indices versus monsoon (Jul-Sep) volumes in acre-feet (af); r is Pearson's linear correlation.

2.3. Step 3. Identify key climatic and atmospheric drivers of the hydrologic opportunity

Understanding the key factors that drive the potential opportunity is critical to understanding its possible role in water management. In step 2, we examined several aspects of the interannual variability of Elephant Butte Reservoir monsoon season volumes. Next we seek to understand the key climate and atmospheric drivers. We recognize that other factors, such as land use and management, are important as well; and though not examined here we discuss this point in the discussion and conclusions. Step 3 analyses rely on several datasets:

- Average precipitation: We use daily precipitation data from PRISM Gridded Climate Data Group (prism.oregonstate.edu), downloadable from http://www.prism.oregonstate.edu/documents/PRISM_downloads_FTP.pdf. Average precipitation is calculated by 1) averaging the daily values over each year's monsoon season (Jul-Sep), and 2) spatially averaging over the Rio Grande watershed contributing to Elephant Butte Reservoir within New Mexico. The data are available through 2014, so the overlapping period with the Elephant Butte Reservoir monsoon volumes is 2000-2014.
- Average large-scale variables: Prein (2018) identifies three potential predictors of monsoon season precipitation anomalies based on weather patterns over New Mexico:

sea level pressure, wind speed, and precipitable water; these are from ECMWF's Interim Reanalysis (Dee et al. 2011) (ERA-Interim) Average values are calculated by 1) averaging the daily values over each year's monsoon season (Jul-Sep), and 2) spatially averaging over the entire state of New Mexico.

In this step, we first examine the runoff efficiency of the Elephant Butte Reservoir monsoon volumes with precipitation (2.3.1). Second, we examine the above 4 predictors (basin-average precipitation, sea level pressure, wind speed, and atmospheric precipitable water) and their linear correlation (Pearson's r) with several monsoon inflow characteristics examined in Step 2 (Section 2.3.2).

2.3.1. Runoff efficiency exhibits interannual variability. Runoff efficiency is calculated as the fraction of runoff, here the Middle Rio Grande monsoon volume (measured as the inflow to Elephant Butte Reservoir), divided by precipitation. Then, we normalize the value (i.e., we divide all values by the maximum runoff efficiency). Figure 7 shows the interannual variability of the runoff efficiency: the black line is calculated using the monsoon total precipitation, and shows that 2006 has the highest normalized efficiency within the years analyzed. To get a sense of the efficiency of the upper part of the distribution and extremes, the efficiency is also shown by using two percentile-based indices derived from the precipitation: PR_P75_{annual} and PR_P99_{annual}, corresponding to the magnitude of the 75^{th} and 99^{th} percentiles of daily precipitation in a given year's monsoon season. All three lines show similar patterns, but the PR_P99_{annual} line (purple) is lower for most years, showing that these heavier precipitation events may be less efficient in most years, except in the most extreme years (e.g., 2006). The $P75_{annual}$ line (orange) is above the black line in some years, indicating the relatively higher efficiency of the top quarter of precipitation days, and is just below the black (and purple) lines in 2006, the most extreme year. This underscores the point that when extremes occur, they can be quite efficient, but that more moderate extremes (e.g., P75) contribute more reliably in any given year.

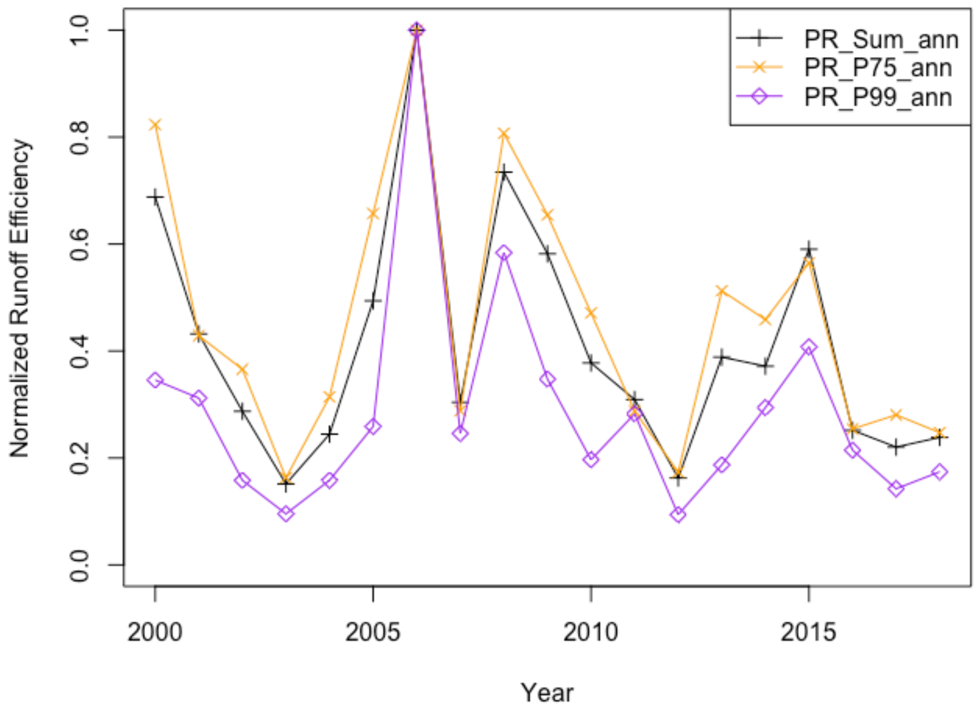

Figure 7. Normalized runoff efficiency of monsoon reservoir volumes using monsoon total precipitation (PR_Sum_ann), and two percentile-based precipitation indices, the magnitude of the year's 75th and 99th percentile precipitation day (PR_P75_ann and PR_P99_ann).

2.3.2. Most monsoon inflow characteristics show strong linear correlations with precipitation and precipitable water. Table 1 shows the linear correlations between the precipitation and large-scale predictors and the monsoon inflow characteristics: total volume and maximum annual inflows, as well as the percentile-based frequency exceedances and annual magnitudes. Table 1 shows that total volumes are most highly correlated with average precipitation over the contributing watershed (r=0.73), and followed by precipitable water (r=0.61). Annual maximum values are most strongly correlated with higher average wind speeds (r=0.52), followed by precipitable water (r=.43), and not significantly correlated with average precipitation, indicating that predictors for averages versus maximums can be quite different. In terms of the frequency characteristics, average precipitation and precipitable water are both important, though as we get to higher percentiles, precipitable water becomes more important. For the frequency of days above P99, sea level pressure also shows a relatively strong association. These initial diagnostics show predictive promise, and the next step is to develop a statistical model to identify the best combination of significant predictors and the associated predictive skill. The appropriate statistical model that will be explored for each characteristic is shown in the last column of Table 1.

Table 1. Pearson's linear correlations (r) between climate and atmospheric predictors and monsoon inflow characteristic predictants for Elephant Butte (EB) Reservoir, as well as the appropriate statistical model form.

Predictant	**Predictors**				**Appropriate Statistical Model Form**
Monsoon EB Inflow Characteristic	**AvgPrecip NM Rio Grande**	**NM Avg Sea Level Pressure**	**NM Avg Precipitable Water**	**NM Avg Wind Speed**	
Total Volume	**0.73**	0.21	**0.61**	-0.26	Linear Regression
Max Annual Inflow	-0.04	-0.15	0.43	0.52	Generalized Extreme Value
Frequency P50	0.53	0.29	0.50	-0.36	Poisson
Frequency P75	**0.73**	0.46	**0.75**	-0.25	Poisson
Frequency P90	**0.77**	0.52	**0.79**	-0.14	Poisson
Frequency P95	**0.83**	0.32	**0.80**	0.11	Poisson
Frequency P99	-0.10	0.47	**0.66**	0.17	Poisson
Magnitude P50_Annual	**0.66**	0.23	0.59	-0.37	Linear Regression
Magnitude P75_Annual	**0.79**	0.28	**0.69**	-0.25	Linear Regression
Magnitude P90_Annual	**0.78**	0.28	**0.63**	-0.05	Linear Regression
Magnitude P95_Annual	0.59	0.23	**0.60**	0.10	Linear Regression
Magnitude P99_Annual	0.24	0.12	0.47	0.25	Linear Regression

2.4. Step 4. Explore the opportunity-management nexus

The fourth step is to explore the opportunity-management nexus, i.e., to identify quantitative and/or qualitative entry-points to test if and how the changing hydrology could impact management decisions. Managers often use local operations models to understand how changes will affect their water storage and key water operations, which can be used to guide their management decisions. In short, it is critical to collaborate with local water managers to understand their decision and modeling context to explore the potential opportunity-management nexus.

For the Rio Grande of New Mexico, the Upper Rio Grande Water Operations Model (URGWOM) includes reservoirs and operation rules to make hydrologic data relevant to management. URGWOM uses streamflow forecasts to select historical hydrographs to calculate inflows into its reservoirs, include Elephant Butte Reservoir. To date, streamflow forecasts are provided by the Natural Resources Conservation Services (NRCS), and are based primarily on snowpack measurements, aiming to predict snowmelt runoff. One potential intersection with this framework is to use the understanding gained here as a launching point to predict a suite of monsoon inflow characteristics. It is hoped that these characteristics could be used as guidance for altering the predicted hydrograph during the monsoon season. The tradeoffs between the best predicted monsoon inflow characteristics (such as the total volume versus the magnitude or frequency attributes) and the ability to integrate with and utility for the URGWOM system need to be evaluated. However, even if the information could not be explicitly integrated in the modeling system, even qualitative information on monsoon inflow characteristics may be useful, and would be more than what is currently provided.

3. Discussion and Conclusions

This study offers a 4-step generalized approach to understanding potential opportunities from changing hydrology, including extremes. We provide a specific a case study example of the Middle Rio Grande basin in New Mexico. The goal is to provide both a general approach and a specific example that can be tailored to other watersheds and management systems.

In this investigation, we examined inflows to Elephant Butte Reservoir during the summer monsoon season, as well their association with average basin precipitation and other large-scale variables. However, we note that water resources in the Western US, including New Mexico, are often over-allocated and tightly managed. With full recognition of this fact, we note that we only focus on climate and atmospheric predictors. We recognize a priori that they will only partially explain the variability in the monsoon inflow characteristics, and presumably some of the remaining, unexplained variability would come from groundwater extraction, land-use changes, land surface characteristics, direct management, as well as other factors not examined here. However, we do note that this approach is more suited to looking at the upper percentiles and extremes, as compared to looking at the lower flows of the distribution, where the non-climate signals would likely be more prevalent.

Demonstrating the generalized framework for the Middle Rio Grande basin in New Mexico offers a successful application of the generalized framework, but we note that there could be other applications that yield less useful, though still informative, results. For example, we also stepped-through parts of the framework for the Pecos River basin, New Mexico, which in terms of infrastructure, is already well set-up for collecting extreme precipitation and subsequent runoff along the system. Here, we were interested in not reservoir inflows, but a decision-relevant variable for this watershed, which is the annual allotment to Carlsbad Irrigation District (CID), a Reclamation Project. The CID allotment is the amount of water the farmers are allowed to take per acre of land irrigated. However, when we examined the connections between the CID and Pecos watershed precipitation and the large-scale circulation variables, we did not find strong associations. This indicates that either a) different explanatory variables may need to be examined for the CID allotment, or b) different decision-relevant variables more closely associated with climate could be examined (e.g., reservoir inflows for this basin).

The provocative question posed in this study was "Extremes of Opportunity?" and the results here suggest several conclusions relevant to water managers. First, it depends on what you define as "extreme". Here, we examine the entire upper half of the flow distribution, and do find that all the upper percentiles contribute a disproportionately higher fraction of the monsoon reservoir volume relative to their occurrence. In the 18-year record examined here, the maximum day contributed 5% of the monsoon flow in that year, and the days that exceeded P99 (or 1% of the days) contributed a median of 32% in the two years that they occurred. Hence, the higher extremes (e.g., maximum and >P99) could certainly provide opportunities in the years they occur. The more moderate extremes (P75-P90) also provide median contributions that are skewed higher than their occurrence, but there is much more variability in these contributions. Nevertheless, we also examined several predictors, including basin-average precipitation and large-scale variables, which showed significant correlations, especially basin-average precipitation and atmospheric precipitable water. These suggest that there is scope for providing outlooks on monsoon inflow characteristics, either from seasonal climate forecasts of the predictor variables, or in terms of downscaling from climate model output. Future work will develop statistical modeling tools to investigate these different applications and to test their ability to integrate with current management in the system.

Acknowledgements

This research was supported by the Bureau of Reclamation Science & Technology award No. 1782: "Detecting, Interpreting, and Modeling Hydrologic Extremes to Support Flexible Water Management and Planning." This material is based upon work supported by the National Center for Atmospheric Research (NCAR), which is a major facility sponsored by the National Science Foundation (NSF) under Cooperative Agreement No. 1852977.

References

Asmerom, Y., Polyak, V.J., Rasmussen, J.B.T., Burns, S.J., and Lachniet, M. 2013. "Multidecadal to multicentury scale collapses of Northern Hemisphere monsoons over the past millennium," PNAS, www.pnas.org/cgi/doi/10.1073/pnas.1214870110

Adams, D.K. and Comrie, A.C. 1997. "The North American monsoon," Bulletin of the American Meteorological Society, 78(10): 2197-2213.

Barnett, T.P., Adam, J.C., and Lettenmaier, D.P. 2005. "Potential impacts of a warming climate on water availability in snow-dominated regions," *Nature*, 438: 303–309.

Chavarria, S. and Gutzler, D.S. 2017. "Observed changes in climate and streamflow in the Upper Rio Grande Basin," Journal of the American Water Works Association, 54(3): 644-659. http://doi.org/10.1111/1752-1688.12640

Collins, M., Knutti, R., Arblaster, J., Dufresne, J.-L., Fichefet, T., Friedlingstein, P., Gao, X., Gutowski, W.J., Johns, T., Krinner, G., Shongwe, M., Tebaldi, C., Weaver, A.J., and Wehner, M. 2013. "Long-term Climate Change: Projections, Commitments and Irreversibility." In: *Climate Change 2013: The Physical Science Basis. Contribution of Working Group I to the Fifth Assessment Report of the Intergovernmental Panel on Climate Change* [Stocker, T.F., Qin, D., Plattner, G.-K., Tignor, M., Allen, S.K., Boschung, J., Nauels, A., Xia, Y., Bex, V., and Midgley, P.M. (eds.)]. Cambridge University Press, Cambridge, UK and New York, NY, USA, pp. 1029-1136.

Dee, D., and Coauthors. 2011. "The ERA-Interim reanalysis: Configuration and performance of the data assimilation system," Quarterly Journal of the Royal Meteorological Society, 137 (656): 553–597.

Douglas, M.W., Maddox, R., Howard, K., and Reyes, S. 1993. "The Mexican monsoon," J. Climate, 6: 1665-1667.

Gutzler, D.S. 2013. “Climate and drought in New Mexico.” In: Water Policy in New Mexico [Brookshire, D.S., Gupta, H.V., and Matthews O.P. (eds.)]. RFF Press, New York, 72–86.

Hayhoe, K., Wuebbles, D.J., Easterling, D.R., Fahey, D.W., Doherty, S., Kossin, J., Sweet, W., Vose, R., and Wehner, M. 2018. “Our Changing Climate.” In *Impacts, Risks, and Adaptation in the United States: Fourth National Climate Assessment, Volume II* [Reidmiller, D.R., Avery, C.W., Easterling, D.R., Kunkel, K.E., Lewis, K.L.M., Maycock, T.K., and Stewart, B.C. (eds.)]. U.S. Global Change Research Program, Washington, DC, USA, pp. 72–144. doi: 10.7930/NCA4.2018.CH2

Kunkel, K. E., Andsager, K., and Easterling, D. D. R. 1999. “Long-Term Trends in Extreme Precipitation Events over the Conterminous United States and Canada,” Journal of Climate, 12(1998): 2515–2527. https://doi.org/10.1175/1520-0442(1999)012<2515:LTTIEP>2.0.CO;2

Lehner, F., Wahl, E.R., Wood, A.W., Blatchford D.B., and Llewellyn, D. 2017. “Assessing recent declines in Upper Rio Grande River runoff efficiency from a paleoclimate perspective.” Geophysical Research Letters, doi:10.1002/2017GL073253.

Mallakpour, I., and Villarini, G. 2017. “Analysis of changes in the magnitude, frequency, and seasonality of heavy precipitation over the contiguous USA,” Theoretical and Applied Climatology, 130(1–2): 345–363. http://doi.org/10.1007/s00704-016-1881-z

Mote, P.W., Hamlet, A.F., Clark, M.P. and Lettenmaier, D.P. 2005. “Declining mountain snowpack in western north America,” Bulletin of the American Meteorological Society, 86, 39–49.

Mote, P.W., Li, S., Lettenmaier, D.P., Xiao M., and Engel, R. 2018. “Dramatic declines in snowpack in the western US,” Npj Climate and Atmospheric Science 1(1), 2, http://doi.org/10.1038/s41612-018-0012-1

Pournasiri Poshtiri, M., Towler, E., Llewellyn, D., and Prein, A.F. 2018. “Extremes of Opportunity: Examining Recent Trends in Warm Season Extreme Precipitation for New Mexico River Basins,” 86th Western Snow Conference, Albuquerque, NM, https://westernsnowconference.org/files/PDFs/2018Poshtiri.pdf.

Prein, A. F. 2019. “The Changing Character of the North American Monsoon and its Impacts on New Mexico's Precipitation,” J. Climate, (in revision).

Seneviratne, S.I., Nicholls, N., Easterling, D., Goodess, C.M., Kanae, S., Kossin, J., Luo, Y., Marengo, J., McInnes, K., Rahimi, M., Reichstein, M., Sorteberg, A., Vera, C., and Zhang, X. 2012. “Changes in climate extremes and their impacts on the natural physical environment.” In: *Managing the Risks of Extreme Events and Disasters to Advance Climate Change Adaptation* [Field, C.B., Barros, V., Stocker, T.F., Qin, D., Dokken, D.J., Ebi, K.L., Mastrandrea, M.D., Mach, K.J., Plattner, G.-K., Allen, S.K., Tignor, M., and Midgley, P.M. (eds.)]. Cambridge University Press, Cambridge, UK, and New York, NY, USA, pp. 109-230.

Serreze, M. C., Clark, M. P., Armstrong, R. L., McGinnis, D. A. and Pulwarty, R. S. 1999. "Characteristics of the western United States snowpack from snowpack telemetry (SNOTEL) data," *Water Resour. Res.,* **35**(7): 2145– 2160.

URGWOM Technical Team. 2005. Draft Upper Rio Grande Water Operations Model Physical Model Documentation: Third Technical Review Committee Draft.

Villarini, G. 2016. "On the seasonality of flooding across the continental United States." *Advances in Water Resources*, *87:* 80–91. http://doi.org/10.1016/j.advwatres.2015.11.009

Wood, K.M. and Ritchie E.A. 2013."An updated climatology of tropical cyclone impacts on the Southwestern United States." Monthly Weather Review, 141: 4322-4336.

Appendix E – Research Products

This Appendix provides a complete list of the research products for each component, including the papers, presentations, and outreach.

The first research component was to examine the variability and trends of precipitation extremes, which resulted in the following products:

- Pournasiri Poshtiri M, Towler E, Llewellyn D, Prein AF (2018) Extremes of Opportunity: Examining Recent Trends in Warm Season Extreme Precipitation for New Mexico River Basins, 86th Western Snow Conference, Albuquerque, NM, https://westernsnowconference.org/files/PDFs/2018Poshtiri.pdf. [Paper]
- Towler E, Llewellyn D, Barrett L, Pournasiri M, Pinson A, Prein A , and Rick Young R (2018) Extremes of Opportunity: Mitigation of Snowmelt Decreases through Improved Management of Local Extreme Precipitation Events, 86th Western Snow Conference, Albuquerque, NM, April 17, 2018. [Poster]
- Pournasiri Poshtiri M, Towler E, Llewellyn D, Prein AF (2020) Recent Trends in Warm Season Extreme Precipitation for the Pecos River Basin. Appendix for Pecos River New Mexico Basin Study. [Paper; in press]
- Pournasiri Poshtiri M, Towler E, Llewellyn D, Prein AF (2018) Extremes of Opportunity: Characterizing the Contribution and Drivers of Monsoon Extreme Streamflows, AGU Annual Conference, Washington, D.C, December 2018. [Poster]

The second component was to identify weather types associated with precipitation anomalies; this resulted in the following paper that is in revision:

- Prein, AF (2019) The Changing Character of the North American Monsoon and its Impacts on New Mexico's Precipitation, Journal of Climate, *in revision*. [Paper]

The third component to statistically model extreme precipitation using the weather type information task has been accepted by a peer-review journal:

- Towler E, Llewellyn D, Prein A, Gilleland E (2019) Extreme-value analysis for the characterization of extremes in water resources: A generalized workflow and case study on New Mexico monsoon precipitation. Weather and Climate Extremes, *accepted*. [Paper]

The fourth component was to develop a generalized framework. Results from this task were presented at the Federal Interagency Sedimentation and Hydrologic Modeling Conference (SEDHYD), as well as published in the associated proceedings:

- Llewellyn D, Towler E, Barrett L, Young R (2019) Extremes of Opportunity? A generalized approach to identify intersections between changing hydrology and water management. Federal Interagency Sedimentation and Hydrologic Modeling Conference (SedHyd), Reno, NV, June 26, 2019. [Presentation]

- Towler E, Llewellyn D, Barrett L, Young R (2019) Extremes of Opportunity? A generalized approach to identify intersections between changing hydrology and water management. Proceedings of the Federal Interagency Sedimentation and Hydrologic Modeling Conference (SEDHYD), Reno, NV, https://www.sedhyd.org/2019/openconf/modules/request.php?module=oc_program&action=view.php&id=160&file=1/160.pdf [Paper]

Outreach to Reclamation, Research, and Water Management Community

Towler E (2019) Extremes of Opportunity? A generalized approach to identify intersections between changing hydrology and water management. S&T Project Team Meeting, Albuquerque Area Office, Albuquerque, NM. May 24, 2019. [Presentation]

Towler E, Llewellyn D, Prein, AF (2019) Extremes of Opportunity? A generalized approach to identify intersections between changing hydrology and water management. S&T Water Operations and Planning Monthly Webinar, January 10, 2019. [Presentation]

Towler E (2018), Detecting, Interpreting, & Modeling Hydrologic Extremes to Support Flexible Water Management and Planning. Seminar to the Hydrometeorology Applications Program (HAP) Research Applications Laboratory (RAL), NCAR, May 18, 2018. [Presentation]

Towler E (2018) Detecting, Interpreting, and Modeling Hydrologic Extremes to Support Flexible Water Management and Planning. All MMM Meeting, NCAR, Boulder, CO, February 8, 2018. [Presentation]

Towler E (2018) Detecting, Interpreting, and Modeling Hydrologic Extremes to Support Flexible Water Management and Planning. Brown Bag Seminar for US Bureau of Reclamation, Remote presentation to Albuquerque Area Office, Albuquerque, NM, January 23, 2018. [Presentation]

Towler E, Llewellyn D, Prein A, Pinson A, Young R, Barrett L (2017) Detecting, Interpreting, and Modeling Hydrologic Extremes to Support Flexible Water Management and Planning. USGS Upper Rio Grande Basin Focus Area Study Project Forum, Remote presentation to Albuquerque, NM, December 4, 2017. [Presentation]

Towler E. (2016) Nonstationary Tools to Detect, Interpret, and Model Hydrologic Extremes to Support Flexible Water Management. Webinar, June 8, 2016. [Webinar presentation to explore research ideas for S&T program with Dagmar Llewellyn and 9 Bureau of Reclamation staff from the Albuquerque Area Office and El Paso Field Office.]

Field Tours

- Upper Rio Grande Tour – Alamosa Office Operations, Reclamation's Closed Basin Project, and San Luis Valley irrigation operations, May 1-3, 2017.